Journal of Organometallic Chemistry, 482 (1994) 207–220

Synthesis and characterisation of metal complexes of ether carbaboranes. Molecular structures of d^6 ML_3, d^8 ML_2 and d^{10} ML complexes of mono- and di-ether C_2B_9 carbaborane ligands, showing the progressive importance of secondary M...O bonding

Kenneth F. Shaw, Bruce D. Reid and Alan J. Welch

Department of Chemistry, University of Edinburgh, Edinburgh EH9 3JJ (UK)

(Received February 10, 1994)

Abstract

The synthesis and characterisation of eight new metal complexes of mono- and di-ether carbaboranes, specifically 1-(CH_2OCH_3)-3-(*p*-cym)-3,1,2-*closo*-$RuC_2B_9H_{10}$, **1**; 1,2-$(CH_2OCH_3)_2$-3-(*p*-cym)-3,1,2-*closo*-$RuC_2B_9H_9$, **2**; $[C_6H_5CH_2NMe_3][1$-(CH_2OCH_3)-3,3-$(CO)_2$-3,1,2-*closo*-$RhC_2B_9H_{10}]$, **3**; 1,2-$(CH_2OCH_3)_2$-3-(cod)-3,1,2-*closo*-$PdC_2B_9H_9$, **4**; 1-(CH_2OCH_3)-3,3-$(Me_2PhP)_2$-3,1,2-*closo*-$PtC_2B_9H_{10}$, **5**; 7,8-$(CH_2OCH_3)_2$-10-*endo*-(Ph_3PHg)-7,8-*nido*-$C_2B_9H_9$, **6**; $[C_6H_5CH_2NMe_3]$ $[(THF)_2La\{C_2B_9H_9(CH_2OCH_3)_2\}_2]$, **7**; and $U\{C_2B_9H_9(CH_2OCH_3)_2\}_2$, **8**, are reported, from the reactions between appropriate metal substrates and either a suspension of $Tl_2[7$-(CH_2OCH_3)-7,8-*nido*-$C_2B_9H_{10}]$ or $Tl_2[7,8$-$(CH_2OCH_3)_2$-7,8-*nido*-$C_2B_9H_9]$, or a THF solution of $Li_2[7,8$-$(CH_2OCH_3)_2$-7,8-*nido*-$C_2B_9H_9]$. The identities and gross structural characteristics of compounds **1–6** are supported by the analysis of IR and multinuclear NMR spectroscopic data, including ^{11}B–^{11}B(COSY) experiments on **4** and **5**. The formulae of the highly air-sensitive compounds **7** and **8** are assigned on the basis of IR and microanalytical data, supported by some NMR studies on **8**. It is proposed that in the THF-free form of this last compound, the ether carbaborane ligands simultaneously π bond (C_2B_3 face) and σ bond (pendant O atom) to the U^{IV} centre. Crystallographic studies of **2**, **5** and two crystalline forms of **6** reveal that, as the formal coordination number of the metal atom decreases, there is increasing interaction between the pendant ether oxygen atom(s) and the metal atom.

Key words: Carboranes; Ruthenium; Rhodium; Palladum; Lanthanum; Uranium; Crystal structure

1. Introduction

There is sustained interest in the chemistries of carbaboranes with functional pendant groups. These species have considerable potential in such diverse areas as precursors for new materials [1] and as boron carriers in neutron-induced tumour therapy [2]. When the pendant group contains donor atoms a rich coordination chemistry can be envisaged. Teixidor et al. [3] have synthesised a variety of metal complexes of *nido* carbaboranes with macrocyclic substituents (O and/or S donor atoms) but in every crystallographically characterised example of these species there is no substantial interaction between the metal centre and the *nido* face of the carbaborane. Interest continues however [4–6] in molecules in which carbaborane ligands do bind facially to a variety of s, p, d and f block metal cations, thereby illustrating the rich diversity of carbametallaborane chemistry.

Recently, we reported a family of mono- and di-ether *closo*-C_2B_{10} carbaboranes and their *nido*-C_2B_9 anions [7], and subsequently demonstrated the coordinating ability of the pendant oxygen atoms in the compound 7,8-$\{CH_2O(CH_3)Li(THF)_2O(CH_3)CH_2\}$-7,8-*nido*-$C_2B_9H_{10}$ [8]. We and others have also shown that coordination of oxygen in a pendant arm to metal atoms already σ-bonded to *closo* carbaboranes is possible [9,10].

We report herein the synthesis and characterisation of a number of d and f block mono- and di-ether carbametallaborane compounds which in some cases

Correspondence to: Prof. A.J. Welch at Department of Chemistry, Heriot-Watt University, Edinborgh EH14 4AS (UK).

0022-328X/94/$7.00
SSDI 0022-328X(94)24611-L

display simultaneous π (C_2B_3 face) and σ (O donor) coordination of ether carbaboranes to metal centres. The d block compounds are identified as ML_n species ($n = 1$–3), where n represents the number of coordination sites occupied by non-polyhedral ligands. It is convenient to discuss structural trends in carbametallaboranes in terms of the orbital number of the $\{ML_n\}$ fragment—the number of fragment orbitals used in cluster bonding. For ML_3 this is 3, for ML_2, 2, and for ML, 1, representing, formally, octahedral, square-planar, and linear metal coordination geometries respectively.

2. Experimental details

2.1. Synthesis and Characterisation

Reactions were generally performed under an atmosphere of dry N_2 by use of standard Schlenk techniques, although some subsequent manipulations were carried out in the open laboratory. Unless otherwise stated, all solvents were dried and distilled under N_2 prior to use. NMR spectra were recorded on Jeol FX90, Bruker WP80SY, WP200SY, or WH360, or Varian VXR600 spectrometers as $CDCl_3$, CD_2Cl_2, $(CD_3)_2CO$ or d_8-THF solutions (generally at 298 K), chemical shifts being reported relative to external $SiMe_4$ (^1H, ^{13}C), $BF_3.OEt_2$ (^{11}B) or 85%H_3PO_4 (^{31}P). Techniques for recording ^{11}B(COSY) spectra have been reported elsewhere [11]. IR spectra were recorded as KBr pellets on a Perkin-Elmer 598 spectrophotometer. C, H and N microanalyses were performed by the departmental service. The starting materials Tl_2[7-(CH_2OCH_3)-7,8-*nido*-$C_2B_9H_{10}$] [7], Tl_2[7,8-(CH_2OCH_3)$_2$-7,8-*nido*-$C_2B_9H_9$] [7], [(*p*-cym)$RuCl_2$]$_2$ [12] (*p*-cym=$C_6H_4Me^iPr$-1,4), $[(CO)_2RhCl]_2$ [13], (cod)$PdCl_2$ [14] (cod=*cyclo*-octa-1,5-diene), $(Me_2PhP)_2PtCl_2$ [15] and $[(Ph_3P)HgCl_2]_2$ [16] were prepared by literature methods or slight variants thereof. [$HNMe_3$][7,8-(CH_2OCH_3)$_2$-7,8-*nido*-$C_2B_9H_{10}$] was made by metathesis of K[7,8-(CH_2OCH_3)$_2$-7,8-*nido*-$C_2B_9H_{10}$] [7] with [$HNMe_3$]Cl and characterised by microanalysis. $La(ClO_4)_3$ and UCl_4 were weighted into Schlenk tubes in a Vacuum Atmospheres He 439 Dri-Train glove box.

2.1.1. 1-(CH_2OCH_3)-3-(p-cym)-3,1,2-closo-$RuC_2B_9H_{10}$ (1)

To a mixture of [(*p*-cym)$RuCl_2$]$_2$ (1.07 g, 1.75 mmol) and Tl_2[7-(CH_2OCH_3)-7,8-*nido*-$C_2B_9H_{10}$] (2.05 g, 3.50 mmol) at −196°C was added CH_2Cl_2 (10 cm^3, degassed). The mixture was allowed to warm to room temperature with stirring. After *ca.* 1 h the mixture was filtered and the deep red filtrate concentrated to *ca.* 2 cm^3 *in vacuo*. Preparative thin layer chromatography on silica, with CH_2Cl_2 as eluant, afforded a fast moving pale-brown band , the product from which was collected and recrystallised by solvent diffusion (CH_2Cl_2 solution : hexane, 1 : 4, −30°C) to yield 1-(CH_2OCH_3)-3-(*p*-cym)-3,1,2-*closo*-$RuC_2B_9H_{10}$, **1**, as large, well-formed crystals.

Yield 0.42 g, 29%. Calculated for $C_{14}H_{29}B_9ORu$; 40.8% C, 7.10% H. Found for **1**; 40.4% C, 6.92% H. IR ν_{max} at 2542 (s, br) (B–H), 1449, 1382, 1124 cm^{-1}. NMR: (CD_2Cl_2) ^1H: δ 5.83 (m, 4H, $CH_{aromatic}$), 3.97 (br s, 1H, CH_{cage}), 3.69 (app. s, 2H, $-CH_2-O$), 3.32 (s, 3H, $O-CH_3$), 2.87 [hept, $^3J_{HH} = 7$ Hz, 1H, $CHMe_2$], 2.31 [s, 3H, $^iPrC_6H_4CH_3$], 1.29 [d, $^3J_{HH} = 7$ Hz, 6H, $CH(CH_3)_2$] ppm. $^{11}B-\{^1H\}$: δ 2.11 [2B, B(8,10)], −2.38 [1B, B(4)], −6.60 [1B, B(7)], −8.93 [2B, B(9,12)], −15.62 [1B, B(5)], −18.19 [1B, B(9)], −19.51 [1B, B(6)] ppm.

2.1.2. 1,2-(CH_2OCH_3)$_2$-3-(p-cym)-3,1,2-closo-$RuC_2B_9H_9$ (2)

[(*p*-cym)$RuCl_2$]$_2$ (0.13 g, 0.22 mmol) and Tl_2[7,8-(CH_2OCH_3)$_2$-7,8-*nido*-$C_2B_9H_9$] (0.35 g, 0.56 mmol) were stirred in CH_2Cl_2 (50 cm^3, degassed) for 40 min, affording a grey precipitate and a red-brown solution. Following filtration, removal of solvent from the filtrate yielded a brown solid. Diffraction-quality single crystals of 1,2-(CH_2OCH_3)$_2$-3-(*p*-cym)-3,1,2-*closo*-$RuC_2B_9H_9$, **2**, were grown by slow diffusion of hexane into a CH_2Cl_2 solution (4 : 1) at −30°C.

Yield 0.09 g, 45%. Calculated for $C_{16}H_{33}B_9O_2Ru$; 42.2% C, 7.25% H. Found for **2**; 42.2% C, 7.20% H. IR ν_{max} at 2648(w), 2583(s, sh), 2540(s, br), 2499 (s, sh), 2484(s, sh) (all B–H), 1440, 1372, 1189, 1088 cm^{-1}. NMR: (CD_2Cl_2) ^1H: δ 5.96 [m, 4H, *H*(32,33,35,36)], 3.85 and 3.72 (AB, $^2J_{HH} = 11.5$ Hz, 4H, $-CH_2-O$), 3.33 (s, 6H, $O-CH_3$), 2.95 [hept, $^3J_{HH} = 7$ Hz, 1H, *H*(341)], 2.30 [s, 3H, C(311)H_3], 1.33 [d, $^3J_{HH} = 7$ Hz, 6H, C(342,343)H_3] ppm. $^{11}B-\{^1H\}$: δ 2.05 [2B, B(8,10)], −2.86 [2B, B(4.7)], −8.73 [2B, B(9,12)], −16.11 [2B, B(5,11)], −19.3 [1B, B(6)] ppm. ^{13}C(DEPT): δ 91.72 and 88.87 (4C, $C_{aromatic}$), 79.07 (2C, $-CH_2-O$), 77.05 [1C, *C*(341)], 59.03 (2C, $O-CH_3$), 30.72 [1C, *C*(311)], 22.49 [2C, *C*(342,343)] ppm.

2.1.3. [$C_6H_5CH_2NMe_3$][1-(CH_2OCH_3)-3,3-$(CO)_2$-3,1,2-closo-$RhC_2B_9H_{10}$] (3)

$[(CO)_2RhCl]_2$ (0.07 g, 0.19 mmol) and Tl_2[7-(CH_2OCH_3)$_2$-7-*nido*-$C_2B_9H_{10}$] (0.22 g, 0.38 mmol) were stirred in THF (15 cm^3, degassed) for 15 min. Solid [$C_6H_5CH_2NMe_3$]Cl (0.07 g, 0.38 mmol) was added and the solution stirred for a further 30 min. After filtration the red-brown solution was concentrated and applied to an alumina column (Bockman activity 2, 15 × 1.5 cm, pre-washed, CH_2Cl_2 :

EtOH[1:1] eluant). A fast moving brown band was collected, from which $[C_6H_5CH_2NMe_3][1\text{-}(CH_2OCH_3)\text{-}3,3\text{-}(CO)_2\text{-}3,1,2\text{-}closo\text{-}RhC_2B_9H_{10}]$, **3**, was afforded as brown microcrystals on recrystallisation (CH_2Cl_2 : hexane, 1:4 by volume) at −30°C.

Yield 0.10 g, 55%. Microanalysis not performed because of loss of service. IR ν_{max} at 2580(m), 2516(s), 2500(s), 2442(m) (all B–H), 2009(s), 1946(s) (both C–O), 1470, 1386, 1158, 1086 cm^{-1}. NMR: ($CDCl_3$) ^1H: δ 7.47 (m, 5H, C_6H_5), 4.44 (s, 2H, $-CH_2-N$), 3.69 and 3.58 (AB, $^2J_{HH}$ = 8.5 Hz, 2H, $-CH_2-O$), 3.26 (s, 3H, $O-CH_3$), 3.10 (s, 9H, $N-CH_3$) ppm. $^{11}B-\{^1H\}$: δ −6.43 (1B), −10.34 (2B), −13.30 (2B), −17.89 (br, 2B), −20.85 (br, 2B) ppm. $^{13}C-\{^1H\}$: δ 189.94 (d, $^1J_{RhC}$ = 76 Hz, 2C, CO), 132.59 (2C, $C_{aromatic}H$), 131.29 (1C, $C_{aromatic}H$), 129.48 (2C, $C_{aromatic}H$), 126.01 (1C, $C_{aromatic}-CH_2$), 78.97 (1C, CH_2-N), 70.33 (1C, $-CH_2-O$), 61.06 (1C, $C_{cage}-CH_2$), 58.37 (1C, $O-CH_3$), 52.92 (3C, $N-CH_3$), 38.87 (1C, $C_{cage}-H$) ppm.

2.1.4. 1,2-$(CH_2OCH_3)_2$-3-(cod)-3,1,2-closo-$PdC_2B_9H_9$ (4)

To a solid mixture of (cod)$PdCl_2$ (0.18 g, 0.65 mmol) and $Tl_2[7,8\text{-}(CH_2OCH_3)_2\text{-}7,8\text{-}nido\text{-}C_2B_9H_9]$ (0.41 g, 0.65 mmol) at −196°C, was added CH_2Cl_2 (10 cm^3, degassed). The mixture was allowed to warm to room temperature with stirring, whereupon it had become almost black. After a further 10 min the mixture was filtered and the filtrate evaporated *in vacuo*. The product was dissolved in the minimum volume of CH_2Cl_2 (*ca.* 4 cm^3) and chromatographed on a Florisil column (100–200 mesh, 17 × 1.5 cm, pre-washed, CH_2Cl_2 eluant). A fast moving purple band was collected and evaporated to dryness *in vacuo*, and the residue then triturated with hexane to afford 1,2-$(CH_2OCH_3)_2$-3-(cod)-3,1,2-*closo*-$PdC_2B_9H_9$, **4**, as a purple air-sensitive solid.

Yield 0.16 g, 57%. Microanalytical data were irreproducible because of decomposition. IR ν_{max} at 2563 (s, v br) (B–H), 1448, 1375, 1102 cm^{-1}. NMR: (CD_2Cl_2) ^1H: δ 5.70 (narrow t, $^3J_{HH}$ < 5 Hz, 4H, $=CH-$), 4.20 and 4.07 (AB, $^2J_{HH}$ = 10.5 Hz, 4H, $-CH_2-O$), 3.49 (s, 6H, $O-CH_3$), 2.60 (narrow d, $^3J_{HH}$ < 5 Hz, 8H, $C-CH_2-$) ppm. $^{11}B-\{^1H\}$: δ 22.90 [1B, B(8)], 0.33 [2B, B(5,11)], −3.94 [1B, B(10)], −5.33 [2B, B(9,12)], −13.74 [2B, B(4,7)], −15.25 [1B, B(6)] ppm: ^{13}C(DEPT): δ 112.22 (2C, $=CH-$), 75.18 (2C, $-CH_2-O$), 58.99 (2C, $O-CH_3$), 30.07 (4C, $C-CH_2-$) ppm.

2.1.5. 1-(CH_2OCH_3)-3,3-$(Me_2PhP)_2$-3,1,2-closo-$PtC_2B_9H_{10}$ (5)

Similarly, $(Me_2PhP)_2PtCl_2$ (0.59 g, 1.09 mmol) and $Tl_2[7\text{-}(CH_2OCH_3)\text{-}7\text{-}nido\text{-}C_2B_9H_{10}]$ (0.64 g, 1.10 mmol) were allowed to warm together in CH_2Cl_2 (12 cm^3). After stirring for 1.5 h at room temperature the grey precipitate and orange solution which had formed were separated by filtration, and the filtrate concentrated to *ca.* 4 cm^3 before being chromatographed on an alumina column (Bockman activity 2 pre-washed with CH_2Cl_2, 9 × 1.5 cm, CH_2Cl_2 eluant). A fast moving yellow-orange band was collected, from which volatiles were removed *in vacuo* to afford an orange solid. Crystallisation by solvent diffusion (CH_2Cl_2 : hexane, 1:6 by volume) at −30°C yielded high quality orange-red crystals of 1-(CH_2OCH_3)-3,3-$(Me_2PhP)_2$-3,1,2-*closo*-$PtC_2B_9H_{10}$, **5**.

Yield 0.52 g, 78%. Calculated for $C_{22}H_{41}B_9O_2P_2Pt$; 42.8% C, 6.65% H. Found for **5**; 42.8% C, 6.63% H. IR ν_{max} at 2576(w, sh), 2558(m, sh), 2520(s), 2439(s, sh) (all B–H), 1431, 1387, 1098 cm^{-1}. NMR at 291 K: (CD_2Cl_2) ^1H: δ 7.38 (m, 10H, C_6H_5), 3.77 (br s, 2H, $-CH_2-O$), 3.46 (s, 3H, $O-CH_3$), 2.95 [br s, 1H, $H(2)$] ppm. $^{11}B-\{^1H\}$: δ 6.52 [1B, B(8), $^1J_{PtB}$ = 254 Hz], −2.60 [1B, B(12)], −6.37 [1B, B(5)], −9.94 [1B, B(10)], −17.17 [2B, B(6,9)], −18.01 [1B, B(11)], −19.79 [2B, B(4,7)] ppm. $^{31}P-\{^1H\}$: δ −12.4 (s) ppm. At 207 K: (CD_2Cl_2) $^{31}P-\{^1H\}$: δ −11.82 and −12.98 (AB, $^2J_{PP}$ = 30 Hz, $^1J_{PtP}$ = 3700 and 3160 Hz respectively) ppm.

2.1.6. 7,8-$(CH_2OCH_3)_2$-10-endo-(Ph_3PHg)-7,8-nido-$C_2B_9H_9$ (6)

Similarly, $Tl_2[7,8\text{-}(CH_2OCH_3)_2\text{-}7,8\text{-}nido\text{-}C_2B_9H_9]$ (0.43 g, 0.69 mmol), $[(Ph_3P)HgCl_2]_2$ (0.37 g, 0.35 mmol) and CH_2Cl_2 (15 cm^3) were slowly brought from −196°C to room temperature, affording a pale yellow filtrate and a grey precipitate. Removal of solvent from the filtrate yielded a soft white solid which was recrystallised from CH_2Cl_2 : hexane by solvent diffusion at −30°C to produce colourless, light-sensitive crystals (α form) of 7,8-$(CH_2OCH_3)_2$-10-*endo*-(Ph_3PHg)-7,8-*nido*-$C_2B_9H_9$, **6**. A second crystalline modification of **6**, the β form, is obtained by cooling a $CDCl_3$ solution to −30°C.

Combined yield 0.41 g, 86%. Calculated for $C_{24}H_{34}B_9HgO_2P$; 42.2% C, 4.98% H. Found for **6**; 41.9% C, 4.92% H. IR ν_{max} at 2573(m), 2542(s), 2520(s), 2500(s), 2479(m), 2435(w) cm^{-1} (all B–H). NMR: ($CDCl_3$) ^1H: δ 7.67 (m, 15H, C_6H_5), 3.35 and 3.27 (AB, $^2J_{HH}$ = 7 Hz, 4H, $-CH_2-O$), 2.74 (s, 6H, $O-CH_3$) ppm: $^{11}B-\{^1H\}$: δ −13.26 (2B), −15.12 (5B), −24.91 (1B), −31.70 (1B) ppm: $^{31}P-\{^1H\}$: δ 55.19 (s) ppm.

2.1.7. $[C_6H_5CH_2NMe_3][(THF)_2La\{C_2B_9H_9(CH_2OCH_3)_2\}_2]$ (7)

To a solution of $[HNMe_3][7,8\text{-}(CH_2OCH_3)_2\text{-}7,8\text{-}nido\text{-}C_2B_9H_{10}]$ (0.35 g, 1.25 mmol) in THF (15 cm^3, degassed) was slowly added two equivalents of *t*BuLi (1.47 cm^3 of a 1.7 M solution in hexane), and the

mixture heated to reflux for 1 h, affording a THF solution of $Li_2[C_2B_9H_9(CH_2OCH_3)_2]$. This solution was stirred with a solution of $La(ClO_4)_3$ in THF (0.27 g, 0.625 mmol; 5 cm^3, degassed) for 2.5 h, followed by addition of a slurry of $[C_6H_5CH_2NMe_3]Cl$ in CH_2Cl_2 (0.29 g, 1.25 mmol; 10 cm^3, degassed). After a further 1 h stirring the mixture was filtered and the filtrate concentrated *in vacuo*. Addition of hexane and cooling to −30°C afforded soft, pale yellow, very air-sensitive crystals of $[C_6H_5CH_2NMe_3][(THF)_2La\{C_2B_9H_9(CH_2OCH_3)_2\}_2]$, **7**.

Calculated for $C_{30}H_{70}B_{18}LaNO_6$; 41.2% C, 8.01% H, 1.60%N. Found for **7**; 42.3% C, 8.67% H, 1.64%N. IR ν_{max} at 2505, 2390 (both B–H), 1470, 1389 cm^{-1}.

2.1.8. $U\{C_2B_9H_9(CH_2OCH_3)_2\}_2$ (8)

To a cold solution of UCl_4 (0.29 g, 0.75 mmol) in THF (10 cm^3, degassed) was added 1.5 mmol of a THF (10 cm^3, degassed) solution of $Li_2[C_2B_9H_9(CH_2OCH_3)_2]$ prepared as above. The mixture was allowed to warm to room temperature, and over a 2 h period it changed from a green solution to a brown solution with grey suspension. The products were separated by filtration and the filtrate divided into two parts. One part was evaporated to dryness *in vacuo* to afford an air-sensitive brown powder, which analysed for the adduct $(THF)_2U\{C_2B_9H_9(CH_2OCH_3)_2\}_2$, **8a**.

Calculated for $C_{20}H_{54}B_{18}O_6U$; 29.2% C, 6.61% H. Found for **8a**; 29.1% C, 6.42% H. IR ν_{max} at 2517 (B–H), 1450, 1383, 1190, 1089, 1011 cm^{-1}.

The other part was concentrated to minimum volume and cooled to −78°C. After *ca.* one week red-orange crystals were recovered, which analysed for the THF-free $U\{C_2B_9H_9(CH_2OCH_3)_2\}_2$, **8b**.

Calculated for $C_{12}H_{28}B_{18}O_4U$; 21.2% C, 5.64% H. Found for **8b**; 20.7% C, 5.05% H.

The ^1H and ^{11}B NMR spectra of **8b** in $(CD_3)_2CO$ were recorded and are discussed in a following section. Several crystals of **8b** were carefully mounted under N_2 in Lindemann capillaries, but none afforded a measurable diffraction pattern.

2.2. Crystallographic Studies

All measurements on **2**, **5**, **6α** and **6β** were carried out at room temperature on an Enraf-Nonius CAD4 diffractometer equipped with graphite-monochromated

TABLE 1. Crystallographic data and details of data collection and structure refinement for **2**, **5**, **6α** and **6β**

	2	**5**	**6α**	**6β**
Crystal size/mm	0.4 × 0.4 × 0.3	0.3 × 0.3 × 0.3	0.3 × 0.2 × 0.2	0.5 × 0.5 × 0.3
Formula	$C_{16}H_{33}B_9O_2Ru$	$C_{22}H_{41}B_9O_2P_2Pt$	$C_{24}H_{34}B_9HgO_2P$	$C_{24}H_{34}B_9HgO_2P$
M	455.79	616.86	683.38	683.38
System	monoclinic	monoclinic	monoclinic	monoclinic
Space group	$P2_1/n$	$P2_1/a$	$P2_1/n$	$P2_1/n$
a/Å	9.7747(20)	18.073(4)	12.617(3)	15.246(5)
b/Å	16.447(5)	11.934(4)	14.616(9)	12.4192(13)
c/Å	13.611(26)	26.344(7)	15.772(9)	16.0393(22)
β/°	93.376(16)	107.241(19)	99.65(4)	111.213(18)
V/Å^3	2184.3	5430.7	2867.4	2831.2
Z	4	8 (2 independent)	4	4
D_{calc}/g cm^{-3}	1.386	1.509	1.583	1.603
μ(Mo–K$_\alpha$)/cm^{-1}	7.12	52.91	54.42	55.11
F(000)/e	936	2424	1336	1336
$\theta_{orientation}$/°	9–11	8–11	9–11	13–14
$\theta_{data\ collection}$/°	1–25	1–25	1–25	1–25
h range	0 → +11	0 → +20	0 → +14	0 → +16
k range	0 → +19	0 → +14	0 → +19	0 → +14
l range	−16 → +16	−31 → +31	−18 → +18	−14 → +14
Data measured	4249	10331	5502	5436
Data observed	3158	7849	4468	4217
Period/hr	107	224	116	116
g	0.000519	0.000314	0.000732	0.000543
R	0.0375	0.0401	0.0386	0.0357
R_w	0.0434	0.0453	0.0469	0.0394
S	1.273	1.041	1.045	1.050
Variables	295	308 per block	392	392
Max. residue/e Å^{-3}	0.59 near O's	0.69 near Pt	1.25 near Hg	0.97 near Hg
Min. residue/e Å^{-3}	−0.70	−0.60	−1.16	−1.06

Mo–K_α X-radiation ($\lambda_{bar} = 0.71069$ Å) operating in the θ–2θ mode.

Table 1 lists details of data collection and structure refinement. In each case the unit cell parameters and orientation matrix for data collection were established by the least-squares refinement of the setting angles of 25 strong, high angle, reflections. Regular measurement of the intensities of check reflections revealed no crystal decay for **2** and **5**. Both crystalline forms of **6**, however, decayed slightly over the data collection period (during which both crystals visibly darkened) and intensities were appropriately adjusted. Only data for which $F \geq 2.0\ \sigma(F)$ were retained for structure solution and refinement.

All four crystal structures were solved by Patterson (metal atom) and difference Fourier (all other non-H atom) methods, and refined by least-squares (full-matrix for **2**, **6**α and **6**β; block-diagonal for **5**, each of two blocks containing the variable parameters of one of the crystallographically independent molecules). An empirical absorption correction (DIFABS [17]) was applied to each data set following isotropic convergence. Phenyl rings were treated as rigid, planar hexagons (C–C 1.395 Å) in **5**, **6**α and **6**β. Cage H atoms were positionally refined from sites located on ΔF maps in each case, whereas all other H atoms were set in idealised positions riding on their bound carbon atom (C–H 1.08 Å). In **2** and **6**β cage H atoms were refined with individual isotropic thermal parameters, whereas these were grouped for the cage H atoms of **5** and **6**α. U values for all other H atoms were refined in groups; 3 for **2**, 2 for **5**, 3 for **6**α and 3 for **6**β. All non-H atoms were refined with anisotropic thermal parameters, and in the final stages of refinement data were weighted such that $w^{-1} = [\sigma^2(F) + gF^2]$.

Atomic scattering factors for B, C, H, O, and P were those inlaid in SHELX76 [18], while those for Ru, Pt and Hg were taked from International Tables [19]. Programs used in addition to those referenced above were CADABS [20], CALC [21], and SHELXTL [22]. Tables of final (non-H) atomic positional parameters appear as Tables 2–5. Tables of thermal parameters and H atoms positions and full lists of bond distances and angles, for all four compounds have been deposited with the Cambridge Crystallographic Data Centre.

TABLE 2. Coordinates of refined non-hydrogen atoms and equivalent isotropic thermal parameters (Å^2) in 1,2-$(CH_2OCH_3)_2$-3-(*p*-cym)-3,1,2-*closo*-$RuC_2B_9H_9$, compound **2**

Atom	x	y	z	U_{eq}
Ru(3)	0.45710(3)	0.12103(2)	0.20778(2)	0.0354(2)
C(31)	0.6108(4)	0.0200(3)	0.2454(4)	0.057(3)
C(32)	0.6082(5)	0.0738(3)	0.3257(4)	0.058(3)
C(33)	0.4845(5)	0.0927(3)	0.3691(3)	0.057(3)
C(34)	0.3589(4)	0.05864(22)	0.3333(3)	0.0451(22)
C(35)	0.3609(4)	0.00628(22)	0.2521(3)	0.0431(22)
C(36)	0.4857(4)	−0.01234(23)	0.2077(3)	0.0466(23)
C(311)	0.7435(5)	−0.0036(4)	0.1999(5)	0.080(4)
C(341)	0.2284(6)	0.0773(3)	0.3843(4)	0.065(3)
C(342)	0.2374(7)	0.0343(3)	0.4845(4)	0.095(4)
C(343)	0.0967(5)	0.0547(3)	0.3243(5)	0.080(4)
C(1)	0.5649(4)	0.21937(24)	0.1386(3)	0.0464(23)
C(11)	0.7107(4)	0.2247(3)	0.1828(4)	0.070(3)
O(1)	0.7817(3)	0.29163(24)	0.1471(4)	0.100(3)
C(12)	0.9209(5)	0.2859(4)	0.1642(5)	0.083(4)
C(2)	0.4293(4)	0.25317(22)	0.2037(3)	0.0396(20)
C(21)	0.4501(5)	0.28686(24)	0.3087(3)	0.0525(25)
O(2)	0.4358(4)	0.37216(18)	0.30977(24)	0.0676(21)
C(22)	0.4410(7)	0.4026(3)	0.4061(4)	0.082(4)
B(4)	0.5088(6)	0.1439(3)	0.0557(4)	0.052(3)
B(5)	0.5377(6)	0.2457(4)	0.0181(4)	0.061(3)
B(6)	0.4920(5)	0.3139(3)	0.1130(4)	0.049(3)
B(7)	0.2830(5)	0.2008(3)	0.1660(3)	0.0396(23)
B(8)	0.3269(5)	0.1316(3)	0.0694(3)	0.0459(25)
B(9)	0.3898(6)	0.1933(3)	−0.0255(4)	0.056(3)
B(10)	0.3814(6)	0.2975(3)	0.0083(4)	0.053(3)
B(11)	0.3146(5)	0.3016(3)	0.1254(4)	0.0436(25)
B(12)	0.2519(5)	0.2282(3)	0.0406(4)	0.048(3)

3. Results and Discussion

3.1. Syntheses and Characterisation

The reaction of $[(p\text{-cym})RuCl_2]_2$ with $Tl_2[7\text{-}(CH_2OCH_3)\text{-}7,8\text{-}nido\text{-}C_2B_9H_{10}]$ and with $Tl_2[7,8\text{-}(CH_2OCH_3)_2\text{-}7,8\text{-}nido\text{-}C_2B_9H_9]$ affords the mono- and di-ether ML_3 carbaruthenaboranes **1** and **2** respectively. The yield of **2** is reasonable, but that of **1** is only modest, this latter species being one of four products of the reaction. However, **1** is easily separated by thin layer chromatography from yellow, pink and orange co-products, all of which are carbaborane-free (IR spectroscopy) and were therefore not pursued.

Compound **1** was characterised by IR and ^1H and $^{11}B/^{11}B\text{-}\{^1H\}$ NMR spectroscopies. ^{13}C(DEPT) NMR spectroscopy was additionally used to identify **2**.

In the ^1H NMR spectrum of **1** the aromatic protons appear as a broad multiplet centred on 5.83 ppm and the cage CH proton resonates at 3.97 ppm. The CH_2 protons in the pendant ether arm have a near-zero chemical shift difference, appearing as a broad singlet centred on 3.69 ppm; other resonances are as expected. In the $^{11}B\text{-}\{^1H\}$ spectrum there are seven peaks in the ratio (high to low frequency) 2:1:1:2:1:1:1. Underlined integrals represent coincidences; the peak at −8.93 ppm. is a true coincidence, while that centred on 2.11 ppm is almost (but not quite) resolved at 64.21 MHz. All resonances show the expected doublet coupling ($^1J_{BH}$ = 120–150 Hz) in the ^{11}B spectrum.

The ^1H NMR spectrum of **2** is very similar to that of **1** except that the ether CH_2 protons give rise to a well-defined AB pattern ($^2J_{HH}$ = 11.5 Hz) and, of

TABLE 3. Coordinates of refined non-hydrogen atoms and equivalent isotropic thermal parameters ($Å^2$) in 1-(CH_2OCH_3)-3,3-($Me_2PhP)_2$-3,1,2-*closo*-$PtC_2B_9H_{10}$, compound **5**

Atom	x	y	z	U_{eq}
C(1A)	0.1369(5)	−0.1302(7)	0.3905(3)	0.046(5)
C(2A)	0.1054(5)	−0.0846(7)	0.4351(3)	0.050(6)
Pt(3A)	0.06436(2)	0.05935(2)	0.36913(1)	0.0346(2)
B(4A)	0.0631(6)	−0.1153(7)	0.3333(3)	0.041(6)
B(5A)	0.0906(7)	−0.2486(8)	0.3655(4)	0.054(7)
B(6A)	0.1214(7)	−0.2290(9)	0.4328(4)	0.059(7)
B(7A)	0.0071(6)	−0.0452(8)	0.4166(4)	0.048(6)
B(8A)	−0.0277(6)	−0.0737(7)	0.3475(4)	0.041(6)
B(9A)	−0.0068(7)	−0.2175(8)	0.3401(4)	0.057(7)
B(10A)	0.0309(7)	−0.2824(8)	0.4026(4)	0.055(7)
B(11A)	0.0441(6)	−0.1747(8)	0.4511(4)	0.051(7)
B(12A)	−0.0396(7)	−0.1757(8)	0.3942(4)	0.055(7)
C(11A)	0.2201(6)	−0.1061(11)	0.3890(5)	0.081(8)
O(1A)	0.2591(5)	−0.0460(8)	0.4289(5)	0.125(9)
C(12A)	0.3364(7)	−0.0299(12)	0.4273(7)	0.167(16)
P(1A)	0.10298(12)	0.21287(18)	0.42263(8)	0.0414(12)
C(32A)	0.2441(3)	0.2511(4)	0.4070(3)	0.064(7)
C(33A)	0.3045(3)	0.3149(4)	0.3992(3)	0.082(9)
C(34A)	0.2982(3)	0.4313(4)	0.3959(3)	0.076(8)
C(35A)	0.2315(3)	0.4840(4)	0.4005(3)	0.075(8)
C(36A)	0.1712(3)	0.4201(4)	0.4084(3)	0.057(6)
C(31A)	0.1775(3)	0.3037(4)	0.4117(3)	0.045(5)
C(4A)	0.0247(5)	0.3051(7)	0.4264(3)	0.052(6)
C(5A)	0.1446(6)	0.1712(7)	0.4918(3)	0.058(6)
P(2A)	0.05184(13)	0.15110(17)	0.29300(8)	0.0426(13)
C(62A)	0.0259(3)	0.3816(5)	0.29221(25)	0.063(7)
C(63A)	−0.0196(3)	0.4761(5)	0.29179(25)	0.083(9)
C(64A)	−0.0977(3)	0.4640(5)	0.28839(25)	0.092(10)
C(65A)	−0.1303(3)	0.3574(5)	0.28540(25)	0.087(9)
C(66A)	−0.0847(3)	0.2628(5)	0.28582(25)	0.065(7)
C(61A)	−0.0066(3)	0.2749(5)	0.28923(25)	0.043(5)
C(7A)	−0.0008(6)	0.0744(7)	0.2350(3)	0.063(6)
C(8A)	0.1377(6)	0.1951(8)	0.2760(4)	0.067(7)
C(1B)	0.3264(5)	0.3647(6)	0.9320(3)	0.043(5)
C(2B)	0.4086(5)	0.4019(7)	0.9352(3)	0.039(5)
Pt(3B)	0.37421(2)	0.28606(2)	0.85494(1)	0.0311(2)
B(4B)	0.2706(5)	0.3760(7)	0.8675(4)	0.037(5)
B(5B)	0.2632(7)	0.4674(8)	0.9205(4)	0.054(7)
B(6B)	0.3548(7)	0.4859(9)	0.9663(4)	0.055(7)
B(7B)	0.4207(5)	0.4628(7)	0.8767(4)	0.040(6)
B(8B)	0.3244(5)	0.4571(7)	0.8286(4)	0.037(5)
B(9B)	0.2634(6)	0.5279(8)	0.8597(4)	0.042(6)
B(10B)	0.3169(7)	0.5900(8)	0.9205(4)	0.051(7)
B(11B)	0.4141(6)	0.5436(8)	0.9318(4)	0.048(6)
B(12B)	0.3575(6)	0.5774(7)	0.8655(4)	0.044(6)
C(11B)	0.3169(6)	0.2675(7)	0.9676(4)	0.064(7)
O(1B)	0.3606(4)	0.1774(5)	0.9626(3)	0.085(6)
C(12B)	0.3499(7)	0.0837(8)	0.9947(4)	0.088(9)
P(1B)	0.30339(12)	0.15986(17)	0.79732(8)	0.0401(12)
C(32B)	0.2154(4)	0.0704(4)	0.85733(25)	0.067(7)
C(33B)	0.1825(4)	−0.0151(4)	0.87959(25)	0.092(9)
C(34B)	0.1937(4)	−0.1268(4)	0.86811(25)	0.093(10)
C(35B)	0.2379(4)	−0.1530(4)	0.83436(25)	0.097(10)
C(36B)	0.2707(4)	−0.0675(4)	0.81210(25)	0.086(9)
C(31B)	0.2595(4)	0.0442(4)	0.82358(25)	0.046(5)
C(4B)	0.3543(6)	0.0940(9)	0.7548(4)	0.070(7)
C(5B)	0.2223(5)	0.2258(7)	0.7492(3)	0.057(6)
P(2B)	0.48992(12)	0.19714(16)	0.86843(9)	0.0417(13)
C(62B)	0.5445(3)	−0.0148(4)	0.85013(21)	0.050(6)
C(63B)	0.5486(3)	−0.1312(4)	0.85481(21)	0.059(6)
C(64B)	0.5032(3)	−0.1875(4)	0.88122(21)	0.065(7)
C(65B)	0.4538(3)	−0.1273(4)	0.90295(21)	0.064(7)
C(66B)	0.4497(3)	−0.0109(4)	0.89827(21)	0.054(6)
C(61B)	0.4950(3)	0.0454(4)	0.87186(21)	0.042(5)
C(7B)	0.5368(6)	0.2371(7)	0.8193(4)	0.073(7)
C(8B)	0.5602(5)	0.2355(8)	0.9309(4)	0.068(7)

course, there is no resonance as a result of cage C*H*. The ^{11}B and $^{11}B-\{^1H\}$ spectra are simplified (2:2:2:2:1) implying time-averaged C_S molecular symmetry (one coincidence) which is also born out by analysis of the ^{13}C(DEPT) spectrum.

The ^{11}B NMR spectra of **1** and **2** were assigned by comparison with that (previously assigned *via* an $^{11}B-^{11}B$ COSY experiment [23]) of 3-(C_6Me_6)-3,1,2-*closo*-$RuC_2B_9H_{11}$, and the relevant data are summarised in Table 6. Replacement of C(H) by C(CH_2OCH_3) has already been shown to result in high frequency shifts of those boron atoms adjacent to the site of substitution [7]. Thus, for example, B(6) in **1** resonates at −19.5 ppm *cf* −24.0 ppm in (C_6Me_6)$RuC_2B_9H_{11}$. In addition, however, antipodal effects [24] are clearly evident, *e.g.* at B(8). B(10) in both **1** and **2** resonates at *ca.* +2 ppm, being accidentally coincident with B(8) in both cases (almost resolved in **1**). Presumably the chemical shift of B(10) is substantially different from that in (C_6Me_6)$RuC_2B_9H_{11}$ because of the change in the nature of the η-bonded arene.

Reaction of $[(CO)_2RhCl]_2$ with Tl_2[7-(CH_2OCH_3)-7,8-*nido*-$C_2B_9H_{10}$], followed by cation metathesis, and of ($Me_2PhP)_2PtCl_2$ with Tl_2[7-(CH_2OCH_3)-7,8-*nido*-$C_2B_9H_{10}$], affords the mono-ether ML_2 carbametallaboranes **3** and **5** respectively, in good yield following chromatographic purification and crystallisation. Similarly, reaction of (cod)$PdCl_2$ with Tl_2[7,8-($CH_2OCH_3)_2$-7,8-*nido*-$C_2B_9H_9$] yields the air-sensitive diether species **4** following work-up involving column chromatography.

At room temperature, compounds **3–5** all show evidence of rapid rotation of the appropriate {ML_2} fragment about an axis from M to the centre of the carbaborane cage. Thus, a single doublet ($^1J_{RhC} = 76$ Hz) resulting from the carbonyl carbon atoms is observed in the ^{13}C NMR spectrum of **3**; only single resonances resulting from both pairs of −C*H*= and −CH_2− (cod) carbon atoms, and only one resonance each for −C*H*= and −CH_2− protons, are recorded in the ^{13}C(DEPT) and ^1H NMR spectra respectively, of **4**; and only a singlet (with ^{195}Pt satellites) is observed in the ^{31}P NMR spectrum of **5**.

TABLE 4. Coordinates of refined non-hydrogen atoms and equivalent isotropic thermal parameters (Å^2) in 7,8-$(CH_2OCH_3)_2$-10-*endo*-(Ph_3PHg)-7,8-*nido*-$C_2B_9H_9$, compound **6** (α modification)

Atom	x	y	z	U_{eq}
Hg(3)	0.07579(2)	0.13499(2)	0.25639(2)	0.0461(2)
C(1)	−0.1315(5)	0.1319(4)	0.3069(3)	0.043(3)
C(2)	−0.1512(5)	0.1449(4)	0.2069(4)	0.044(3)
B(4)	−0.0388(6)	0.1998(5)	0.3568(4)	0.045(4)
B(5)	−0.1773(7)	0.2233(5)	0.3575(5)	0.057(5)
B(6)	−0.2509(6)	0.1822(5)	0.2606(5)	0.055(4)
B(7)	−0.0753(5)	0.2247(5)	0.1744(4)	0.042(4)
B(8)	0.0043(6)	0.2718(4)	0.2744(4)	0.044(4)
B(9)	−0.0914(6)	0.3102(5)	0.3363(4)	0.049(4)
B(10)	−0.2239(7)	0.2989(6)	0.2755(5)	0.059(5)
B(11)	−0.2125(6)	0.2469(5)	0.1775(5)	0.052(4)
B(12)	−0.1150(6)	0.3254(5)	0.2216(4)	0.049(4)
C(11)	−0.1389(5)	0.0367(4)	0.3450(4)	0.056(4)
O(1)	−0.0362(4)	−0.0053(3)	0.3556(3)	0.058(3)
C(12)	−0.0325(7)	−0.0825(5)	0.4104(5)	0.077(5)
C(21)	−0.1824(5)	0.0644(4)	0.1485(4)	0.049(4)
O(2)	−0.0866(4)	0.0198(3)	0.1341(3)	0.059(3)
C(22)	−0.1064(7)	−0.0462(5)	0.0667(4)	0.070(5)
P(1)	0.20623(12)	0.01788(10)	0.24850(9)	0.0405(8)
C(32)	0.2782(3)	0.1365(3)	0.1343(3)	0.066(5)
C(33)	0.3527(3)	0.1708(3)	0.0863(3)	0.087(6)
C(34)	0.4563(3)	0.1344(3)	0.0970(3)	0.087(6)
C(35)	0.4854(3)	0.0638(3)	0.1558(3)	0.077(5)
C(36)	0.4109(3)	0.0295(3)	0.2038(3)	0.063(4)
C(31)	0.3073(3)	0.0658(3)	0.1930(3)	0.044(3)
C(42)	0.2081(3)	−0.1204(3)	0.12620(25)	0.053(4)
C(43)	0.1742(3)	−0.2041(3)	0.08851(25)	0.062(4)
C(44)	0.0940(3)	−0.2539(3)	0.11889(25)	0.068(5)
C(45)	0.0478(3)	−0.2201(3)	0.18698(25)	0.074(5)
C(46)	0.0818(3)	−0.1365(3)	0.22467(25)	0.061(4)
C(41)	0.1620(3)	−0.0867(3)	0.19428(25)	0.043(3)
C(52)	0.2670(3)	0.04943(22)	0.42207(24)	0.054(4)
C(53)	0.3201(3)	0.02903(22)	0.50475(24)	0.062(4)
C(54)	0.3744(3)	−0.05394(22)	0.52081(24)	0.064(4)
C(55)	0.3756(3)	−0.11652(22)	0.45419(24)	0.075(5)
C(56)	0.3224(3)	−0.09612(22)	0.37150(24)	0.063(4)
C(51)	0.2682(3)	−0.01315(22)	0.35544(24)	0.045(3)

TABLE 5. Coordinates of refined non-hydrogen atoms and equivalent isotropic thermal parameters (Å^2) in 7,8-$(CH_2OCH_3)_2$-10-*endo*-(Ph_3PHg)-7,8-*nido*-$C_2B_9H_9$, compound **6** (β modification)

Atom	x	y	z	U_{eq}
Hg(3)	0.16090(1)	0.05923(2)	0.47862(1)	0.0399(1)
C(1)	0.2038(4)	−0.1225(4)	0.3833(3)	0.039(3)
C(2)	0.1063(3)	−0.1504(4)	0.3901(3)	0.036(3)
B(4)	0.2831(4)	−0.0804(5)	0.4775(4)	0.040(4)
B(5)	0.2892(5)	−0.2144(6)	0.4401(5)	0.048(4)
B(6)	0.1739(5)	−0.2569(5)	0.3801(4)	0.045(4)
B(7)	0.1049(4)	−0.1285(5)	0.4893(4)	0.041(4)
B(8)	0.2250(5)	−0.0846(5)	0.5596(4)	0.041(4)
B(9)	0.3022(5)	−0.1889(5)	0.5513(4)	0.045(4)
B(10)	0.2330(5)	−0.3005(5)	0.4907(5)	0.052(4)
B(11)	0.1146(5)	−0.2621(5)	0.4541(5)	0.049(4)
B(12)	0.1882(5)	−0.2192(5)	0.5595(4)	0.048(4)
P(1)	0.16021(9)	0.24872(11)	0.44735(9)	0.0337(8)
C(11)	0.2044(4)	−0.0734(5)	0.2976(4)	0.053(4)
O(1)	0.1698(3)	0.0324(3)	0.2930(3)	0.058(3)
C(12)	0.1531(6)	0.0819(6)	0.2099(5)	0.082(6)
C(21)	0.0173(4)	−0.1334(5)	0.3086(4)	0.048(4)
O(2)	−0.0218(3)	−0.0346(4)	0.3149(4)	0.077(4)
C(22)	−0.1104(5)	−0.0184(7)	0.2451(6)	0.089(6)
C(32)	0.32222(25)	0.2133(3)	0.4116(3)	0.053(4)
C(33)	0.41407(25)	0.2351(3)	0.4178(3)	0.066(5)
C(34)	0.46104(25)	0.3252(3)	0.4647(3)	0.062(4)
C(35)	0.41615(25)	0.3937(3)	0.5056(3)	0.069(5)
C(36)	0.32430(25)	0.3719(3)	0.4994(3)	0.054(4)
C(31)	0.27733(25)	0.2817(3)	0.4525(3)	0.037(3)
C(42)	0.16711(24)	0.27752(21)	0.61944(21)	0.042(3)
C(43)	0.16359(24)	0.33829(21)	0.69124(21)	0.050(4)
C(44)	0.13594(24)	0.44596(21)	0.67873(21)	0.052(4)
C(45)	0.11181(24)	0.49286(21)	0.59442(21)	0.049(4)
C(46)	0.11534(24)	0.43209(21)	0.52262(21)	0.043(3)
C(41)	0.14299(24)	0.32443(21)	0.53512(21)	0.033(3)
C(52)	0.10314(24)	0.3790(4)	0.2966(3)	0.075(5)
C(53)	0.03873(24)	0.4135(4)	0.2146(3)	0.098(7)
C(54)	−0.04933(24)	0.3645(4)	0.1787(3)	0.074(5)
C(55)	−0.07298(24)	0.2811(4)	0.2248(3)	0.086(6)
C(56)	−0.00858(24)	0.2466(4)	0.3068(3)	0.065(5)
C(51)	0.07948(24)	0.2956(4)	0.3427(3)	0.036(3)

Spectroscopic parameters [ν_{CO}, $\delta(^{13}C)$] of the carbonyl groups in **3** are in close similarity with those previously reported [25] for the analogue [1,2-Me_2-3,3-$(CO)_2$-3,1,2-*closo*-$RhC_2B_9H_9]^-$. The ^{11}B NMR spectrum of **3** yields only five resonances (four of integral 2 must be because of coincidences) and has not been assigned.

In contrast, the ^{11}B spectrum of **4** shows no coincidences and has been assigned by an ^{11}B–^{11}B(COSY) experiment. Of particular note is the high frequency chemical shift (+22.9 ppm) of B(8), the central boron atom in the metal-bonded ligand face. Since B(8) is antipodal to B(6), and B(6) in **4** resonates *ca.* 8 ppm to higher frequency than that in 3-(cod)-3,1,2-*closo*-$PdC_2B_9H_{11}$ [26], a low frequency shift relative to the B(8) resonance in the unsubstituted analogue (+17.7 ppm) might have been anticipated. The observed high frequency resonance could imply [26] a substantial metal-slipped [27] structure for **4**, possibly arising from the steric influence of the two ether substituents, but it

TABLE 6. Comparison of ^{11}B NMR chemical shifts (ppm) in carbaruthenaboranes

Boron atom	$(C_6Me_6)RuC_2B_9H_{11}$ [23]	1	2
B(6)	4.2	2.1	2.0
B(10)	−2.3	2.1	2.0
B(4)	−5.4	−2.4	−2.9
B(7)	−5.4	−6.6	−2.9
B(9)	−9.5	−8.9	−8.7
B(12)	−9.5	−8.9	−8.7
B(5)	−19.8	−15.6	−16.1
B(11)	−19.8	−18.2	−16.1
B(6)	−24.0	−19.5	−19.3

should always be remembered that correlations between B(8) chemical shift and slip parameter are best treated with caution [28].

The ^{11}B NMR shifts of the carbaplatinaborane **5** were also assigned by analysis of a correlated spectrum. Signals at *ca.* −17.2 ppm and −19.8 ppm each represent coincidences, and that at +6.5 ppm shows well-defined satellites because of coupling to ^{195}Pt, $^{1}J_{PtB}$ = 254 Hz. Again, this highest frequency resonance is assigned to B(8). As previously noted, the ^{31}P NMR spectrum of **5** at room temperature is consistent with rapid rotation of the $\{PtP_2\}$ fragment relative to the cage. At *ca.* 260 K this fluctionality is just arrested, and at 207 K the spectrum consists of a well-resolved AB pattern (with ^{195}Pt satellites) because of inequivalent phosphorus atoms, with a mutual PP coupling of 30 Hz.

The di-ether ML carbametallaborane **6** is afforded in excellent yield by reaction between $[(Ph_3P)HgCl_2]_2$ and $Tl_2[7,8\text{-}(CH_2OCH_3)_2\text{-}7,8\text{-}nido\text{-}C_2B_9H_9]$. Compound **6**, which may be obtained in two modifications (α and β, see later) as colourless, photosensitive crystals, was characterised by IR and multinuclear NMR spectroscopies. Absorptions associated with B–H stretch in the IR spectrum of **5** are unusually well-resolved, there being six (the exact number of symmetry-independent boron atoms) identifiable peaks between 2775 and 2435 cm^{-1}. In the ^{1}H NMR spectrum the methyl protons of the ether functions resonate at unusually low frequency, 2.74 ppm. The ^{11}B spectrum is consistent with C_S molecular symmetry and shows a triple (2 + 2 + 1) coincidence at −15.1 ppm.

One of our prime reasons for developing ether carbaboranes was to produce ligands capable of stabilising *f* block metal cations, either through coordination by the ether oxygen atom(s) (σ) or by the carbaborane ligand face (π) or both simultaneously.

When $La(ClO_4)_3$ reacts with $Li_2[7,8\text{-}(CH_2OCH_3)_2\text{-}7,8\text{-}nido\text{-}C_2B_9H_9]$ in THF, compound **7** is produced as an air-sensitive crystalline material, formulated as the bis(THF) adduct on the basis of microanalysis. Crystals of **7** proved to be very soft, and none survived mounting, even at low temperatures, for crystallographic analysis. In the absence of such a study, the mode of coordination of the carbaborane ligands to the lanthanum centre remains unknown. However, the presence of six O donor atoms per La means that a reasonable metal coordination number can be attained without the need for facial (π) bonding by either ether carbaborane, and in that respect **7** may possess structural aspects which resemble those of the crystallographically characterised [8] species $7,8\text{-}\{CH_2O(CH_3)Li(THF)_2O(CH_3)CH_2\}\text{-}7,8\text{-}nido\text{-}C_2B_9H_{10}$.

The reaction between $Li_2[7,8\text{-}(CH_2OCH_3)_2\text{-}7,8\text{-}nido\text{-}C_2B_9H_9]$ and UCl_4 in THF affords the neutral bis(carbaborane) uranium species **8**. Surprisingly, it appears that **8** can be obtained as the bis(THF) adduct **8a** by evaporation of a THF solution, but as the THF-free **8b** by slow crystallisation from THF. The ^{1}H and ^{11}B NMR spectra of **8b** in $(CD_3)_2CO$ were recorded. Although the observation (^{11}B) of resonances assigned to $[7,8\text{-}(CH_2OCH_3)_2\text{-}7,8\text{-}nido\text{-}C_2B_9H_{10}]^-$ and $B(OH)_3$ suggested some decomposition, several additional peaks were clearly visible well outside the normal diamagnetic ranges of both nuclei. In the ^{1}H spectrum broad (B*H*) peaks at frequencies as high as 78 ppm and as low as −37 ppm, and sharp (ether–*H*) resonances between 46 ppm and −65 ppm, were observed, and in the ^{11}B spectrum (broad) signals at frequencies as high as 140 ppm were evident. Clearly, these chemical shift ranges are consistent with involvement of the carbaborane ligand with the paramagnetic (f^2) metal centre. On the basis that **8b** is relatively oxygen deficient we tentatively suggest simultaneous σ (O) and π (C_2B_3 face) coordination by the ether carbaborane(s), at least in this case—it is impossible to envisage a reasonable uranium coordination sphere without such ligation. Unfortunately, although crystals of **8b** were able to be successfully transferred to a diffractometer, none yielded discrete reflections.

3.2. Structural Studies

The solid-state molecular structures of compounds **2**, **5** and **6** (both α and β forms) were determined *via* crystallographic study, these compounds representing examples of d^6 ML_3, d^8 ML_2 and d^{10} ML ether

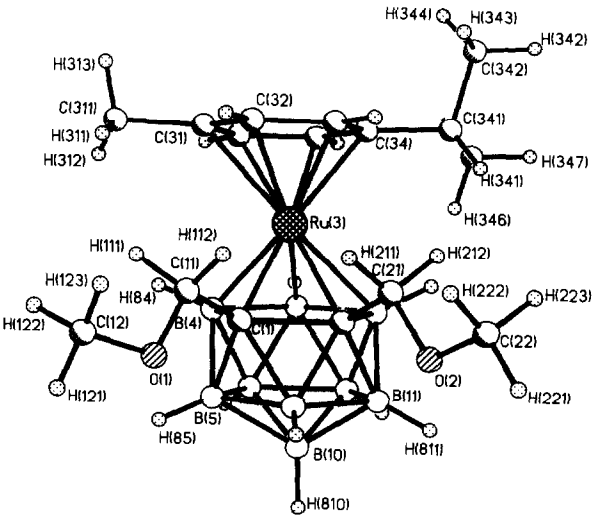

Fig. 1. Perspective view of the molecular structure of **2** with sufficient atoms labelling to completely identify all atoms. Note the "O-down" orientation of both pendant ether groups.

TABLE 7. Interatomic distances (Å) and selected interbond angles (°) in **2**

Ru(3)–C(31)	2.278(5)	B(4)–B(5)	1.778(8)
Ru(3)–C(32)	2.254(5)	B(4)–B(8)	1.810(7)
Ru(3)–C(33)	2.245(4)	B(4)–B(9)	1.755(8)
Ru(3)–C(34)	2.256(4)	B(5)–B(6)	1.788(8)
Ru(3)–C(35)	2.208(4)	B(5)–B(9)	1.755(8)
Ru(3)–C(36)	2.211(4)	B(5)–B(10)	1.748(8)
Ru(3)–C(1)	2.175(4)	B(6)–B(10)	1.757(7)
Ru(3)–C(2)	2.191(4)	B(6)–B(11)	1.763(7)
Ru(3)–B(4)	2.192(5)	B(7)–B(8)	1.810(6)
Ru(3)–B(7)	2.197(4)	B(7)–B(11)	1.781(6)
Ru(3)–B(8)	2.217(5)	B(7)–B(12)	1.774(7)
C(31)–C(311)	1.521(7)	B(8)–B(9)	1.780(7)
C(34)–C(341)	1.519(6)	B(8)–B(12)	1.783(7)
C(341)–C(342)	1.534(8)	B(9)–B(10)	1.788(8)
C(341)–C(343)	1.529(8)	B(9)–B(12)	1.760(8)
C(1)–C(11)	1.517(6)	B(10)–B(11)	1.758(7)
C(1)–C(2)	1.730(5)	B(10)–B(12)	1.777(7)
C(1)–B(4)	1.744(7)	B(11)–B(12)	1.756(7)
C(1)–B(5)	1.702(7)		
C(1)–B(6)	1.738(6)		
C(11)–O(1)	1.403(6)		
O(1)–C(12)	1.370(7)		
C(2)–C(21)	1.535(6)		
C(2)–B(6)	1.729(6)		
C(2)–B(7)	1.722(6)		
C(2)–B(11)	1.699(6)		
C(21)–O(2)	1.410(5)		
O(2)–C(22)	1.401(7)		
C(31)–Ru(3)–C(32)	36.19(17)	B(5)–B(4)–B(9)	59.6(3)
C(31)–Ru(3)–C(36)	36.37(15)	B(8)–B(4)–B(9)	59.9(3)
C(32)–Ru(3)–C(33)	36.56(17)	C(1)–B(5)–B(4)	60.1(3)
C(33)–Ru(3)–C(34)	36.50(15)	C(1)–B(5)–B(6)	59.7(3)
C(34)–Ru(3)–C(35)	36.60(14)	B(4)–B(5)–B(9)	59.6(3)
C(35)–Ru(3)–C(36)	37.65(14)	B(6)–B(5)–B(10)	59.6(3)
C(1)–Ru(3)–C(2)	46.68(14)	B(9)–B(5)–B(10)	61.0(3)
C(1)–Ru(3)–B(4)	47.07(17)	C(1)–B(6)–C(2)	59.87(25)
C(2)–Ru(3)–B(7)	46.20(15)	C(1)–B(6)–B(5)	57.7(3)
B(4)–Ru(3)–B(8)	48.47(18)	C(2)–B(6)–B(11)	58.2(3)
B(7)–Ru(3)–B(8)	48.40(17)	B(5)–B(6)–B(10)	59.1(3)
C(32)–C(31)–C(311)	122.1(4)	B(10)–B(6)–B(11)	59.9(3)
C(36)–C(31)–C(311)	120.0(4)	B(8)–B(7)–Ru(3)	66.38(21)
C(33)–C(34)–C(341)	120.0(4)	Ru(3)–B(7)–C(2)	66.69(19)
C(35)–C(34)–C(341)	122.4(4)	C(2)–B(7)–B(11)	58.01(24)
C(34)–C(341)–C(342)	107.9(4)	B(8)–B(7)–B(12)	59.7(3)
C(34)–C(341)–C(343)	114.2(4)	B(11)–B(7)–B(12)	59.2(3)
C(342)–C(341)–C(343)	111.4(4)	Ru(3)–B(8)–B(4)	65.04(22)
C(11)–C(1)–C(2)	120.6(3)	Ru(3)–B(8)–B(7)	65.23(20)
C(11)–C(1)–B(4)	123.4(4)	B(4)–B(8)–B(9)	58.5(3)
C(11)–C(1)–B(5)	117.2(4)	B(7)–B(8)–B(12)	59.2(3)
C(11)–C(1)–B(6)	113.1(3)	B(9)–B(8)–B(12)	59.2(3)
Ru(3)–C(1)–C(2)	67.13(18)	B(4)–B(9)–B(5)	60.9(3)
C(2)–C(1)–B(4)	66.98(22)	B(4)–B(9)–B(8)	61.6(3)
B(4)–C(1)–B(5)	62.1(3)	B(5)–B(9)–B(10)	59.3(3)
B(5)–C(1)–B(6)	62.6(3)	B(8)–B(9)–B(12)	60.5(3)
B(6)–C(1)–C(2)	59.81(25)	B(10)–B(9)–B(12)	60.3(3)
C(1)–C(11)–O(1)	112.4(4)	B(5)–B(10)–B(6)	61.3(3)
C(11)–O(1)–C(12)	113.2(4)	B(5)–B(10)–B(9)	59.7(3)
C(21)–C(2)–C(1)	122.0(3)	B(6)–B(10)–B(11)	60.2(3)
C(21)–C(2)–B(6)	115.0(3)	B(9)–B(10)–B(12)	59.4(3)
C(21)–C(2)–B(7)	121.4(3)	B(11)–B(10)–B(12)	59.5(3)
C(21)–C(2)–B(11)	117.5(3)	C(2)–B(11)–B(6)	59.9(3)

TABLE 7. Continued

B(7)–C(2)–Ru(3)	67.11(19)	C(2)–B(11)–B(7)	59.26(24)
Ru(3)–C(2)–C(1)	66.19(18)	B(6)–B(11)–B(10)	59.9(3)
C(1)–C(2)–B(6)	60.32(25)	B(7)–B(11)–B(12)	60.2(3)
B(6)–C(2)–B(11)	61.9(3)	B(10)–B(11)–B(12)	60.8(3)
B(7)–C(2)–B(11)	62.7(3)	B(7)–B(12)–B(8)	61.2(3)
C(2)–C(21)–O(2)	111.1(3)	B(7)–B(12)–B(11)	60.6(3)
C(21)–O(2)–C(22)	111.5(4)	B(8)–B(12)–B(9)	60.3(3)
B(8)–B(4)–Ru(3)	66.49(22)	B(9)–B(12)–B(10)	60.3(3)
Ru(3)–B(4)–C(1)	65.95(22)	B(10)–B(12)–B(11)	59.7(3)
C(1)–B(4)–B(5)	57.8(3)		

carbametallaboranes, respectively. Interest particularly attends any changes in involvement of the pendant ether oxygen atom(s) with the (facially bound) metal atoms as a consequence of increasing coordinative unsaturation.

Figure 1 shows a perspective view of compound **2** and Table 7 lists the determined interatomic distances and selected interbond angles. Compound **2** possesses a coordinatively saturated d^6 metal centre and hence no Ru...O interaction is expected or observed. This species therefore serves as a suitable reference against which to discuss the other ether carbametallaboranes.

The Ru atom is more or less centrally situated over the carbaborane C_2B_3 face (slip parameter 0.013 Å [27]). The *p*-cymene ligand is asymmetrically disposed with respect to the carbaborane, although clearly these ligands are able to rotate relative to each other in

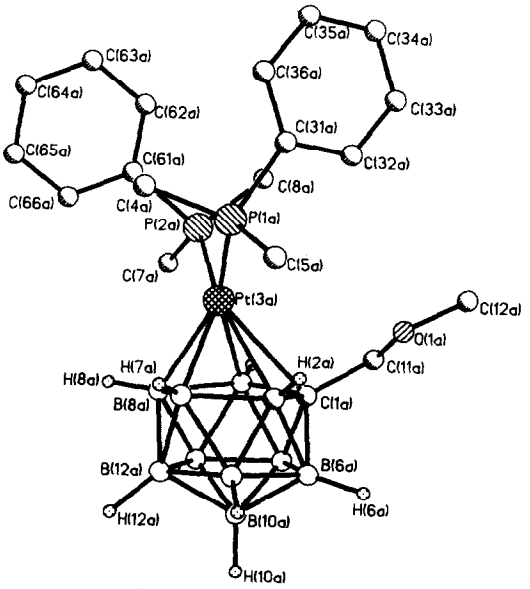

Fig. 2. Perspective view of a single molecule of **5A**, adopting the same atom shading conventions as Fig. 1. H atoms associated with the phosphine ligands are not shown for clarity. The ether group adopts an "O flat" position.

solution at room temperature, since time-averaged C_S molecular symmetry is evident from ^{11}B and ^{13}C NMR spectroscopies. The arene ring and the C_2B_3 face are inclined at an angle of 7.0°, with C(32) and C(33) furthest away. Only part of this tilt may be ascribed to the stronger *trans* influence of boron over carbon in carbametallaboranes [29,30], because corresponding tilt angles in 3-(C_6H_6)-3,1,2-*closo*-$RuC_2B_9H_{11}$ and 3-(C_6Me_6)-3,1,2-*closo*-$RuC_2B_9H_{11}$ are only 2.3° and 2.1° respectively [30,31]. That there is some degree of *p*-cymene/ether crowding in the solid-state is evidenced from measured H...H contacts less than or close to the appropriate van der Waals sum [H(111)...H(311) 2.24 Å; H(112)...H(332) 2.47 Å; H(212)...H(333) 2.54; H(212)...H(341) 2.52 Å] in spite of the arene ring tilt and the relative depression of the ether groups [C(11) and C(21) subtend elevation angles with respect to the lower B_5 girdle of 22.5° and 23.8° respectively]. Similar congestion between pendant ether groups and an η-bonded exopolyhderal ligand has been noted in 1,2-$(CH_2OCH_3)_2$-3-(C_9H_7)-3,1,2-*closo*-$CoC_2B_9H_9$ [32]. The ether functions in **2** define C_{cage}–C_{cage}–CH_2–O torsion angles of −100.2° and −105.7° respectively ("O down"), which position O(1) and O(2) as far as possible from Ru(3), and are mutually crowded, with H(112)...H(211) 2.01 Å and C(1)–C(2) relatively long at 1.730(5) Å.

Compound **5**, an ether carbaborane complex of a d^8 ML_2 centre, crystallises with two independent molecules (**A** and **B**) in the asymmetric fraction of the unit cell. Perspective views of each of these are given in Figs. 2 and 3 respectively, and Tables 8 and 9 list interatomic distances and relevant interbond angles.

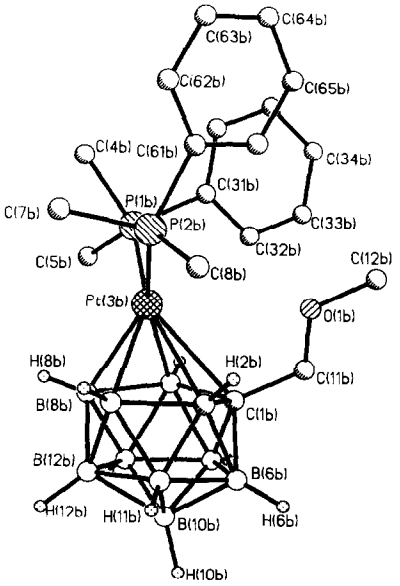

Fig. 3. Molecular structure of **5B**, again with phosphine H atoms removed. Note the "O up" orientation.

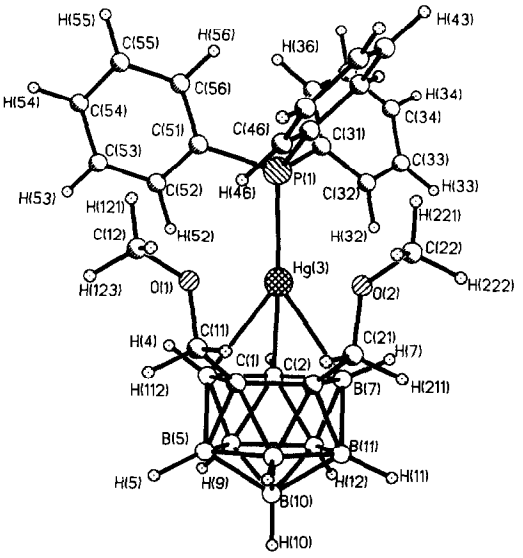

Fig. 4. Perspective view of compound **6** in the α crystallographic modification. Note that for the carbametallaborane cage a *closo* numbering convention is adopted. Both ether groups are "O up".

In **5** the carbaborane is mono(C)substituted and the PtP_2 plane is consequently twisted away from the conformation observed [27] in 3,3-$(Et_3P)_2$-3,1,2-*closo*-$PtC_2B_9H_{11}$ to lie, in both **5A** and **5B**, nearly perpendicular to the plane passing through C(1), B(10) and B(12). A similar orientation is observed in 1-Ph-3,3-$(Me_2PhP)_2$-3,1,2-*closo*-$PtC_2B_9H_{10}$ [33] and is sterically induced [34]. In **5**, however, there is some evidence [35] that mono-ether substitution modifies the frontier molecular orbitals of the carbaborane in such a way that the observed conformations are, at least partially, electronically preferred.

Structurally, molecules **5A** and **5B** essentially differ in the orientation of one of the phosphine ligands and in the C(2)–C(1)–C(11)–O torsion angle. In **5A** the latter is only 1.6°, and there is evidence for an intramolecular O(1a)...H(2a) interaction, 2.58(8) Å [H(2a) is relatively protonic] *cf* the reciprocal intermolecular hydrogen bonding in the solid-state structure [8] of 1-(CH_2OCH_3)-1,2-*closo*-$C_2B_{10}H_{11}$. In this "O flat" orientation there is no involvement of O(1a) with Pt(3a), Pt... > 3.6 Å. In contrast, in **5B** the C(2)–C(1)–C(11)–O torsion is 51.9° ("O up") which positions O(1b) only 3.197(7) Å from Pt(3b). We interpret this as an indication of (albeit very weak) secondary interaction [36,37] between the ether oxygen atom and the metal centre.

Firmer evidence of such interactions is afforded by consideration of the molecular structures of **6**α and **6**β. In both crystalline modifications of this (d^{10} ML)

TABLE 8. Interatomic distances (Å) in **5A** and **5B**

C(1A)–C(2A)	1.550(12)	B(6A)–H(6A)	1.16(7)
C(1A)–B(4A)	1.702(13)	B(7A)–B(8A)	1.776(14)
C(1A)–B(5A)	1.676(14)	B(7A)–B(11A)	1.816(15)
C(1A)–B(6A)	1.703(14)	B(7A)–B(12A)	1.785(15)
C(1A)–C(11A)	1.542(15)	B(7A)–H(7A)	1.01(7)
C(2A)–Pt(3A)	2.401(9)	B(8A)–B(9A)	1.780(15)
C(2A)–B(6A)	1.752(15)	B(8A)–B(12A)	1.789(15)
C(2A)–B(7A)	1.762(14)	B(8A)–H(8A)	1.09(7)
C(2A)–B(11A)	1.685(14)	B(9A)–B(10A)	1.764(16)
C(2A)–H(2A)	0.84(8)	B(9A)–B(12A)	1.769(16)
Pt(3A)–B(4A)	2.286(10)	B(9A)–H(9A)	1.07(7)
Pt(3A)–B(7A)	2.228(10)	B(10A)–B(11A)	1.778(16)
Pt(3A)–B(8A)	2.247(10)	B(10A)–B(12A)	1.768(16)
Pt(3A)–P(1A)	2.2912(22)	B(10A)–H(10A)	1.18(7)
Pt(3A)–P(2A)	2.2381(22)	B(11A)–B(12A)	1.786(15)
B(4A)–B(5A)	1.802(15)	B(11A)–H(11A)	1.28(7)
B(4A)–H(4A)	1.11(7)	B(12A)–H(12A)	1.24(7)
B(4A)–B(8A)	1.856(14)	C(11A)–O(1A)	1.295(16)
B(4A)–B(9A)	1.802(15)	O(1A)–C(12A)	1.423(19)
B(5A)–B(6A)	1.712(16)	P(1A)–C(31A)	1.818(6)
B(5A)–B(9A)	1.728(16)	P(1A)–C(4A)	1.818(9)
B(5A)–B(10A)	1.705(16)	P(1A)–C(5A)	1.823(9)
B(5A)–H(5A)	1.10(7)	P(2A)–C(61A)	1.802(6)
B(6A)–B(10A)	1.715(16)	P(2A)–C(7A)	1.795(10)
B(6A)–B(11A)	1.733(16)	P(2A)–C(8A)	1.816(10)
C(1B)–C(2B)	1.527(12)	B(6B)–H(6B)	1.11(7)
C(1B)–B(4B)	1.707(12)	B(7B)–B(8B)	1.826(13)
C(1B)–B(5B)	1.641(14)	B(7B)–B(11B)	1.776(14)
C(1B)–B(6B)	1.702(14)	B(7B)–B(12B)	1.750(14)
C(1B)–C(11B)	1.534(13)	B(7B)–H(7B)	1.14(7)
C(2B)–Pt(3B)	2.448(8)	B(8B)–B(9B)	1.771(14)
C(2B)–B(6B)	1.759(14)	B(8B)–B(12B)	1.738(14)
C(2B)–B(7B)	1.774(12)	B(8B)–H(8B)	1.03(7)
C(2B)–B(11B)	1.698(13)	B(9B)–B(10B)	1.772(15)
C(2B)–H(2B)	1.05(7)	B(9B)–B(12B)	1.763(14)
Pt(3B)–B(4B)	2.266(9)	B(9B)–H(9B)	0.87(7)
Pt(3B)–B(7B)	2.281(10)	B(10B)–B(11B)	1.781(15)
Pt(3B)–B(8B)	2.255(9)	B(10B)–B(12B)	1.816(15)
Pt(3B)–P(1B)	2.2498(21)	B(10B)–H(10B)	1.09(7)
Pt(3B)–P(2B)	2.2770(22)	B(11B)–B(12B)	1.790(14)
B(4B)–B(5B)	1.808(14)	B(11B)–H(11B)	1.02(7)
B(4B)–B(8B)	1.877(13)	B(12B)–H(12B)	1.13(7)
B(4B)–B(9B)	1.825(14)	C(11B)–O(1B)	1.364(12)
B(4B)–H(4B)	1.04(7)	O(1B)–C(12B)	1.448(14)
B(5B)–B(6B)	1.750(16)	P(1B)–C(31B)	1.827(7)
B(5B)–B(9B)	1.760(15)	P(1B)–C(4B)	1.825(10)
B(5B)–B(10B)	1.756(15)	P(1B)–C(5B)	1.809(9)
B(5B)–H(5B)	0.98(7)	P(2B)–C(61B)	1.814(6)
B(6B)–B(10B)	1.726(15)	P(2B)–C(7B)	1.810(10)
B(6B)–B(11B)	1.739(15)	P(2B)–C(8B)	1.816(10)

di-ether carbamercuraborane (see Figs. 4 and 5, and Tables 10 and 11) both ether functions occupy "O up" positions [appropriate torsion angles about C(11)–O(1) and C(21)–O(2) of 89.7° and 86.6° for **6**α, 70.7° and 96.3° for **6**β], resulting in Hg(3)...O contacts of 3.065(4), 3.070(4), 3.050(4) and 3.376(5) Å respectively. Note that although **6** is strictly a *nido* species with the

TABLE 9. Selected interbond angles (°) in **5A** and **5B**

C(2A)–C(1A)–B(6A)	65.0(6)	B(5A)–B(9A)–B(10A)	58.4(6)
C(2A)–C(1A)–C(11A)	122.3(8)	B(8A)–B(9A)–B(12A)	60.5(6)
B(4A)–C(1A)–B(5A)	64.5(6)	B(10A)–B(9A)–B(12A)	60.1(6)
B(4A)–C(1A)–C(11A)	118.2(7)	B(5A)–B(10A)–B(6A)	60.1(7)
B(5A)–C(1A)–B(6A)	60.9(6)	B(5A)–B(10A)–B(9A)	59.7(6)
B(5A)–C(1A)–C(11A)	121.6(8)	B(6A)–B(10A)–B(11A)	59.5(6)
B(6A)–C(1A)–C(11A)	119.8(8)	B(9A)–B(10A)–B(12A)	60.1(6)
C(1A)–C(2A)–B(6A)	61.7(6)	B(11A)–B(10A)–B(12A)	60.5(6)
B(6A)–C(2A)–B(11A)	60.5(6)	C(2A)–B(11A)–B(6A)	61.6(6)
B(7A)–C(2A)–B(11A)	63.6(6)	C(2A)–B(11A)–B(7A)	60.3(6)
C(2A)–Pt(3A)–B(7A)	44.5(3)	B(6A)–B(11A)–B(10A)	58.5(6)
C(2A)–Pt(3A)–P(1A)	98.83(23)	B(7A)–B(11A)–B(12A)	59.4(6)
C(2A)–Pt(3A)–P(2A)	158.04(23)	B(10A)–B(11A)–B(12A)	59.5(6)
B(4A)–Pt(3A)–B(8A)	48.3(3)	B(7A)–B(12A)–B(8A)	59.6(6)
B(4A)–Pt(3A)–P(1A)	161.37(24)	B(7A)–B(12A)–B(11A)	61.1(6)
B(4A)–Pt(3A)–P(2A)	95.13(25)	B(8A)–B(12A)–B(9A)	60.0(6)
B(7A)–Pt(3A)–B(8A)	46.8(4)	B(9A)–B(12A)–B(10A)	59.8(6)
P(1A)–Pt(3A)–P(2A)	95.29(8)	B(10A)–B(12A)–B(11A)	60.0(6)
B(5A)–B(4A)–B(9A)	57.3(6)	C(1A)–C(11A)–O(1A)	112.5(10)
B(8A)–B(4A)–B(9A)	58.2(6)	C(11A)–O(1A)–C(12A)	110.7(11)
C(1A)–B(5A)–B(4A)	58.5(6)	Pt(3A)–P(1A)–C(31A)	118.93(22)
C(1A)–B(5A)–B(6A)	60.4(6)	Pt(3A)–P(1A)–C(4A)	114.7(3)
B(4A)–B(5A)–B(9A)	61.4(6)	Pt(3A)–P(1A)–C(5A)	111.0(3)
B(6A)–B(5A)–B(10A)	60.3(7)	C(31A)–P(1A)–C(4A)	105.9(3)
B(9A)–B(5A)–B(10A)	61.8(7)	C(31A)–P(1A)–C(5A)	102.5(4)
C(1A)–B(6A)–C(2A)	53.3(5)	C(4A)–P(1A)–C(5A)	102.0(4)
C(1A)–B(6A)–B(5A)	58.8(6)	P(1A)–C(31A)–C(32A)	116.4(5)
C(2A)–B(6A)–B(11A)	57.8(6)	P(1A)–C(31A)–C(36A)	123.6(5)
B(5A)–B(6A)–B(10A)	59.7(7)	Pt(3A)–P(2A)–C(61A)	110.63(22)
B(10A)–B(6A)–B(11A)	62.1(7)	Pt(3A)–P(2A)–C(7A)	113.7(3)
C(2A)–B(7A)–B(11A)	56.2(6)	Pt(3A)–P(2A)–C(8A)	119.8(3)
B(8A)–B(7A)–B(12A)	60.3(6)	C(61A)–P(2A)–C(7A)	102.5(4)
B(11A)–B(7A)–B(12A)	59.5(6)	C(61A)–P(2A)–C(8A)	106.2(4)
B(4A)–B(8A)–B(9A)	59.4(6)	C(7A)–P(2A)–C(8A)	102.3(4)
B(7A)–B(8A)–B(12A)	60.1(6)	P(2A)–C(61A)–C(62A)	121.0(5)
B(9A)–B(8A)–B(12A)	59.4(6)	P(2A)–C(61A)–C(66A)	119.0(5)
B(4A)–B(9A)–B(5A)	61.3(6)	C(62A)–C(61A)–C(66A)	120.0(6)
B(4A)–B(9A)–B(8A)	62.4(6)		
C(2B)–C(1B)–B(6B)	65.7(6)	B(5B)–B(9B)–B(10B)	59.6(6)
C(2B)–C(1B)–C(11B)	118.1(7)	B(8B)–B(9B)–B(12B)	58.9(5)
B(4B)–C(1B)–B(5B)	65.3(6)	B(10B)–B(9B)–B(12B)	61.8(6)
B(4B)–C(1B)–C(11B)	122.0(7)	B(5B)–B(10B)–B(6B)	60.4(6)
B(5B)–C(1B)–C(6B)	63.1(6)	B(5B)–B(10B)–B(9B)	59.9(6)
B(5B)–C(1B)–C(11B)	118.6(7)	B(6B)–B(10B)–B(11B)	59.4(6)
B(6B)–C(1B)–C(11B)	112.9(7)	B(9B)–B(10B)–B(12B)	58.8(6)
C(1B)–C(2B)–B(6B)	61.9(6)	B(11B)–B(10B)–B(12B)	59.7(6)
B(6B)–C(2B)–B(11B)	60.4(6)	C(2B)–B(11B)–B(6B)	61.5(6)
B(7B)–C(2B)–B(11B)	61.5(5)	C(2B)–B(11B)–B(7B)	61.4(5)
C(2B)–Pt(3B)–B(7B)	43.9(3)	B(6B)–B(11B)–B(10B)	58.7(6)
C(2B)–Pt(3B)–P(1B)	155.42(20)	B(7B)–B(11B)–B(12B)	58.8(6)
C(2B)–Pt(3B)–P(2B)	98.18(20)	B(10B)–B(11B)–B(12B)	61.2(6)
B(4B)–Pt(3B)–B(8B)	49.1(3)	B(7B)–B(12B)–B(8B)	63.1(6)
B(4B)–Pt(3B)–P(1B)	94.96(24)	B(7B)–B(12B)–B(11B)	60.2(6)
B(4B)–Pt(3B)–P(2B)	163.40(24)	B(8B)–B(12B)–B(9B)	60.8(6)
B(7B)–Pt(3B)–B(8B)	47.5(3)	B(9B)–B(12B)–B(10B)	59.3(6)
P(1B)–Pt(3B)–P(2B)	96.08(8)	B(10B)–B(12B)–B(11B)	59.2(6)
B(5B)–B(4B)–B(9B)	58.0(6)	C(1B)–C(11B)–O(1B)	111.4(8)
B(8B)–B(4B)–B(9B)	57.1(5)	C(11B)–O(1B)–C(12B)	111.8(8)
C(1B)–B(5B)–B(4B)	59.1(6)	Pt(3B)–P(1B)–C(31B)	118.28(22)
C(1B)–B(5B)–B(6B)	60.2(6)	Pt(3B)–P(1B)–C(4B)	114.4(3)

TABLE 9. Continued

B(4B)–B(5B)–B(9B)	61.5(6)	Pt(3B)–P(1B)–C(5B)	111.3(3)
B(6B)–B(5B)–B(10B)	59.0(6)	C(31B)–P(1B)–C(4B)	105.1(4)
B(9B)–B(5B)–B(10B)	60.5(6)	C(31B)–P(1B)–C(5B)	104.0(4)
C(1B)–B(6B)–C(2B)	52.3(5)	C(4B)–P(1B)–C(5B)	102.0(4)
C(1B)–B(6B)–B(5B)	56.7(6)	P(1B)–C(31B)–C(32B)	117.8(5)
C(2B)–B(6B)–B(11B)	58.1(6)	P(1B)–C(31B)–C(36B)	122.2(5)
B(5B)–B(6B)–B(10B)	60.7(6)	Pt(3B)–P(2B)–C(61B)	120.24(20)
B(10B)–B(6B)–B(11B)	61.9(6)	Pt(3B)–P(2B)–C(7B)	111.6(3)
C(2B)–B(7B)–B(11B)	57.2(5)	Pt(3B)–P(2B)–C(8B)	112.8(3)
B(8B)–B(7B)–B(12B)	58.1(5)	C(61B)–P(2B)–C(7B)	105.7(4)
B(11B)–B(7B)–B(12B)	61.0(6)	C(61B)–P(2B)–C(8B)	101.3(4)
B(4B)–B(8B)–B(9B)	60.0(5)	C(7B)–P(2B)–C(8B)	103.5(5)
B(7B)–B(8B)–B(12B)	58.7(5)	P(2B)–C(61B)–C(62B)	121.5(4)
B(9B)–B(8B)–B(12B)	60.3(6)	P(2B)–C(61B)–C(66B)	118.5(4)
B(4B)–B(9B)–B(5B)	60.5(6)	C(62B)–C(61B)–C(66B)	120.0(5)
B(4B)–B(9B)–B(8B)	62.9(5)		

$HgPPh_3$ unit *endo* σ-bonded to the central boron atom of the cage face, a *closo* numbering scheme is deliberately used to facilitate comparisons with **2** and **5**. These Hg...O distances, particularly the first three, should be compared with similar contacts in $PhHg(C_9H_6NO)$ [38] of 3.3–3.4 Å, where the Hg...O interactions are considered weak, and those in PhHgOAc [39] of 2.85–3.13 Å where Hg...O is considered significant. In 1-(CH_3Hg)-2-$(CH_2OCH_2CH_3)_2$-1,2-*closo*-$C_2B_{10}H_{10}$ [10], $Hg–O_{ether}$ is 2.75 Å and is generally regarded as a substantial bond.

The Hg...O interactions in **6** and related species presumably involve (in localised terminology) donation from an occupied oxygen 2p or ⟨2p–2s⟩ hybrid orbital to vacant 6p orbital(s) on mercury, and such bonding would be expected to result in a number of structural

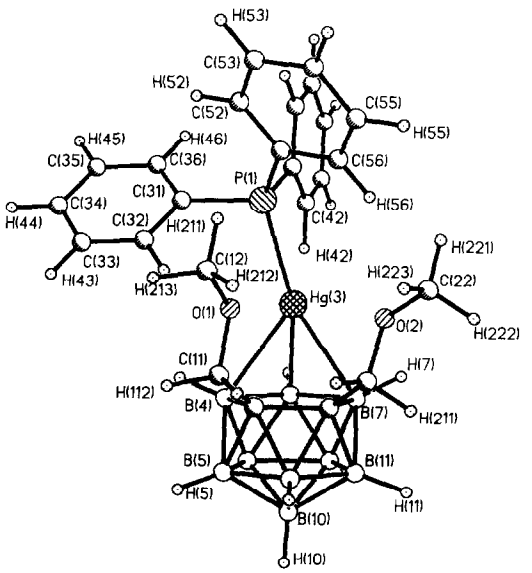

Fig. 5. View of a molecule of **6** in the β crystal in the same direction as for Fig. 4. Again, ether groups are "O up", but note, in addition, the tilted phosphine ligand.

TABLE 10. Interatomic distances (Å) and selected interbond angles (°) in **6α**

Hg(3)–B(4)	2.502(7)	B(8)–B(9)	1.766(10)
Hg(3)–B(7)	2.490(7)	B(8)–B(12)	1.776(10)
Hg(3)–B(8)	2.231(7)	B(9)–B(10)	1.790(11)
Hg(3)–P(1)	2.3922(15)	B(9)–B(12)	1.796(10)
C(1)–C(2)	1.565(8)	B(10)–B(11)	1.751(11)
C(1)–B(4)	1.633(9)	B(10)–B(12)	1.776(11)
C(1)–B(5)	1.706(10)	B(11)–B(12)	1.740(11)
C(1)–B(6)	1.725(10)	C(11)–O(1)	1.418(8)
C(1)–C(11)	1.524(9)	O(1)–C(12)	1.417(9)
C(2)–B(6)	1.719(10)	C(21)–O(2)	1.423(8)
C(2)–B(7)	1.645(9)	O(2)–C(22)	1.427(9)
C(2)–B(11)	1.708(10)	P(1)–C(31)	1.805(5)
C(2)–C(21)	1.506(8)	P(1)–C(41)	1.794(4)
B(4)–B(5)	1.782(11)	P(1)–C(51)	1.794(4)
B(4)–B(8)	1.824(10)		
B(4)–B(9)	1.755(10)		
B(5)–B(6)	1.757(11)		
B(5)–B(9)	1.738(11)		
B(5)–B(10)	1.728(12)		
B(6)–B(10)	1.748(12)		
B(6)–B(11)	1.749(11)		
B(7)–B(8)	1.855(10)		
B(7)–B(11)	1.769(10)		
B(7)–B(12)	1.760(10)		
B(4)–Hg(3)–B(7)	69.89(22)	B(11)–B(7)–B(12)	59.1(4)
B(4)–Hg(3)–B(8)	44.87(24)	B(4)–B(8)–B(9)	58.5(4)
B(7)–Hg(3)–B(8)	45.87(24)	B(7)–B(8)–B(12)	57.9(4)
B(4)–Hg(3)–P(1)	141.19(17)	B(9)–B(8)–B(12)	60.9(4)
B(7)–Hg(3)–P(1)	145.41(16)	B(4)–B(9)–B(5)	61.4(4)
C(2)–C(1)–B(5)	111.6(5)	B(4)–B(9)–B(8)	62.4(4)
C(2)–C(1)–B(6)	62.8(4)	B(5)–B(9)–B(10)	58.6(4)
C(2)–C(1)–C(11)	119.9(5)	B(8)–B(9)–B(12)	59.8(4)
B(4)–C(1)–B(6)	116.7(5)	B(10)–B(9)–B(12)	59.4(4)
B(4)–C(1)–C(11)	116.8(5)	B(5)–B(10)–B(6)	60.7(5)
B(5)–C(1)–B(6)	61.6(4)	B(5)–B(10)–B(9)	59.2(4)
B(5)–C(1)–C(11)	118.8(5)	B(6)–B(10)–B(11)	60.0(5)
B(6)–C(1)–C(11)	116.7(5)	B(9)–B(10)–B(12)	60.5(4)
C(1)–C(2)–B(11)	111.6(5)	B(11)–B(10)–B(12)	59.1(4)
B(6)–C(2)–B(11)	61.4(4)	C(2)–B(11)–B(6)	59.6(4)
B(6)–C(2)–C(21)	114.3(5)	C(2)–B(11)–B(7)	56.4(4)
B(7)–C(2)–B(11)	63.7(4)	B(6)–B(11)–B(10)	59.9(5)
B(7)–C(2)–C(21)	118.0(5)	B(7)–B(11)–B(12)	60.2(4)
B(11)–C(2)–C(21)	117.1(5)	B(10)–B(11)–B(12)	61.2(4)
C(1)–B(4)–B(5)	59.7(4)	B(7)–B(12)–B(8)	63.3(4)
B(5)–B(4)–B(9)	58.9(4)	B(7)–B(12)–B(11)	60.7(4)
B(8)–B(4)–B(9)	59.1(4)	B(8)–B(12)–B(9)	59.3(4)
C(1)–B(5)–B(4)	55.8(4)	B(9)–B(12)–B(10)	60.1(4)
C(1)–B(5)–B(6)	59.7(4)	B(10)–B(12)–B(11)	59.7(4)
B(4)–B(5)–B(9)	59.8(4)	Hg(3)–P(1)–C(31)	107.19(15)
B(6)–B(5)–B(10)	60.2(5)	Hg(3)–P(1)–C(41)	118.18(14)
B(9)–B(5)–B(10)	62.2(5)	Hg(3)–P(1)–C(51)	109.09(14)
C(1)–B(6)–C(2)	54.1(4)	C(31)–P(1)–C(41)	106.77(20)
C(1)–B(6)–B(5)	58.7(4)	C(31)–P(1)–C(51)	108.79(20)
C(2)–B(6)–B(11)	59.0(4)	C(41)–P(1)–C(51)	106.54(19)
B(5)–B(6)–B(10)	59.1(5)	C(1)–C(11)–O(1)	109.1(5)
B(10)–B(6)–B(11)	60.1(5)	C(11)–O(1)–C(12)	110.7(5)
C(2)–B(7)–B(11)	59.9(4)	C(2)–C(21)–O(2)	108.3(5)
B(8)–B(7)–B(12)	58.8(4)	C(21)–O(2)–C(22)	112.4(5)

features, the recognition of which therefore adds validity to the suggestion of such bonding. Thus, for example, P–Hg...O angles close to 90° are anticipated, and

TABLE 11. Interatomic distances (Å) and selected interbond angles (°) in **6β**

Hg(3)–B(4)	2.551(6)	B(7)–B(8)	1.853(9)
Hg(3)–B(7)	2.511(7)	B(7)–B(11)	1.777(10)
Hg(3)–B(8)	2.218(7)	B(7)–B(12)	1.766(10)
Hg(3)–P(1)	2.4062(14)	B(8)–B(9)	1.787(10)
C(1)–C(2)	1.568(8)	B(8)–B(12)	1.764(10)
C(1)–B(4)	1.643(8)	B(9)–B(10)	1.799(10)
C(1)–B(5)	1.724(9)	B(9)–B(12)	1.829(10)
C(1)–B(6)	1.726(9)		
C(1)–C(11)	1.509(8)	B(10)–B(11)	1.750(11)
C(2)–B(6)	1.720(9)	B(10)–B(12)	1.802(10)
C(2)–B(7)	1.624(8)	B(11)–B(12)	1.741(10)
C(2)–B(11)	1.703(9)	P(1)–C(31)	1.806(4)
C(2)–C(21)	1.521(8)	P(1)–C(41)	1.791(4)
B(4)–B(5)	1.783(10)	P(1)–C(51)	1.783(5)
B(4)–B(8)	1.835(9)	C(11)–O(1)	1.409(5)
B(4)–B(9)	1.748(10)	O(1)–C(12)	1.406(9)
B(5)–B(6)	1.752(10)	C(21)–O(2)	1.384(8)
B(5)–B(9)	1.751(10)	O(2)–C(22)	1.423(10)
B(5)–B(10)	1.744(10)		
B(6)–B(10)	1.761(10)		
B(6)–B(11)	1.735(10)		
B(4)–Hg(3)–B(7)	68.68(21)	B(11)–B(7)–B(12)	58.9(4)
B(4)–Hg(3)–B(8)	44.57(22)	B(4)–B(8)–B(9)	57.7(4)
B(7)–Hg(3)–B(8)	45.62(23)	B(7)–B(8)–B(12)	58.4(4)
B(4)–Hg(3)–P(1)	127.73(15)	B(9)–B(8)–B(12)	62.0(4)
B(7)–Hg(3)–P(1)	161.27(15)	B(4)–B(9)–B(5)	61.3(4)
C(2)–C(1)–B(5)	111.8(4)	B(4)–B(9)–B(8)	62.5(4)
C(2)–C(1)–B(6)	62.7(4)	B(5)–B(9)–B(10)	58.8(4)
C(2)–C(1)–C(11)	118.2(5)	B(8)–B(9)–B(12)	58.4(4)
B(4)–C(1)–B(6)	115.7(4)	B(10)–B(9)–B(12)	59.6(4)
B(4)–C(1)–C(11)	117.7(5)	B(5)–B(10)–B(6)	60.0(4)
B(5)–C(1)–B(6)	61.1(4)	B(5)–B(10)–B(9)	59.2(4)
B(5)–C(1)–C(11)	119.8(5)	B(6)–B(10)–B(11)	59.2(4)
B(6)–C(1)–C(11)	116.9(5)	B(9)–B(10)–B(12)	61.1(4)
C(1)–C(2)–B(11)	110.9(4)	B(11)–B(10)–B(12)	58.7(4)
B(6)–C(2)–B(11)	60.9(4)	C(2)–B(11)–B(6)	60.0(4)
B(6)–C(2)–C(21)	113.9(4)	C(2)–B(11)–B(7)	55.6(4)
B(7)–C(2)–B(11)	64.5(4)	B(6)–B(11)–B(10)	60.7(4)
B(7)–C(2)–C(21)	119.7(5)	B(7)–B(11)–B(12)	60.3(4)
B(11)–C(2)–C(21)	118.7(5)	B(10)–B(11)–B(12)	62.2(4)
C(1)–B(4)–B(5)	60.3(4)	B(7)–B(12)–B(8)	63.3(4)
B(5)–B(4)–B(9)	59.5(4)	B(7)–B(12)–B(11)	60.9(4)
B(8)–B(4)–B(9)	59.8(4)	B(8)–B(12)–B(9)	59.6(4)
C(1)–B(5)–B(4)	55.8(4)	B(9)–B(12)–B(10)	59.4(4)
C(1)–B(5)–B(6)	59.5(4)	B(10)–B(12)–B(11)	59.2(4)
B(4)–B(5)–B(9)	59.3(4)	Hg(3)–P(1)–C(31)	106.44(13)
B(6)–B(5)–B(10)	60.5(4)	Hg(3)–P(1)–C(41)	109.91(12)
B(9)–B(5)–B(10)	62.0(4)	Hg(3)–P(1)–C(51)	117.74(15)
C(1)–B(6)–C(2)	54.1(3)	C(31)–P(1)–C(41)	105.63(17)
C(1)–B(6)–B(5)	59.4(4)	C(31)–P(1)–C(51)	107.66(19)
C(2)–B(6)–B(11)	59.1(4)	C(41)–P(1)–C(51)	108.76(19)
B(5)–B(6)–B(10)	59.5(4)	C(1)–C(11)–O(1)	107.4(5)
B(10)–B(6)–B(11)	60.1(4)	C(11)–O(1)–C(12)	113.2(5)
C(2)–B(7)–B(11)	59.9(4)	C(2)–C(21)–O(2)	109.6(5)
B(8)–B(7)–B(12)	58.3(4)	C(21)–O(2)–C(22)	112.3(6)

are indeed observed for the three short Hg...O contacts, being 85.86(9)°, 88.15(9)° and 84.35(9)° to $O(1)_{6\alpha}$, $O(2)_{6\alpha}$ and $O(1)_{6\beta}$ respectively, *cf* 104.04(10)° to $O(2)_{6\beta}$.

Other measurable parameters, which can be discussed for the whole series of ether carbametallaboranes, include (i) the M...O–C angles, expected to be closest when O → M donation is strongest and (ii) elevation angles of the substituent ether groups, which may exceed the icosahedral ideal of 26° to maximise O → M interaction. We find that the difference in M...O–C angles is 43.9–55.2° in **6** [the greatest involving O(2) of **6β**], 64.9° in **5B** and 73.4° in **5A**. Ether elevation angles (with respect to the lower B_5 pentagon) are 30.6–26.7° in **6** [the lowest being to C(2) of **6α**] and less than 26° in all other cases, the measurement of such angles in excess of 26° for non-H substituents of a carbametallaborane being an extremely rare occurence. Moreover, additional evidence for Hg...O interactions in **6** derives from the fact that both molecules exhibit reduced metal slipping (0.78 Å and 0.88 Å for **6α** and **6β**) relative to that (0.92 Å) in 10-*endo*-(Ph_3PHg)-7,8-*nido*-$C_2B_9H_{11}$ [40]. Substitution at the cage carbon atoms in related species has previously been shown to afford a sterically-induced increase in the slip parameter, *e.g* to 1.10 Å in 7,8-Ph_2-10-*endo*-(Ph_3PHg)-7,8-*nido*-$C_2B_9H_9$ [41].

Finally, we note that the phosphine ligand in **6β** is measureably tilted to one side (compare Figs. 4 and 5) rendering P–Hg–B(7) greater than P–Hg–B(4) by *ca.* 33°. The crystal packings of **6α** and **6β** have been analysed in detail [35] and full discussion is outside the intended scope of this contribution. Suffice it to say that in the crystal of **6β**, which is the more dense of the two modifications, a phenyl group of one molecule fits tightly between two phenyl groups and the two ether pendants of another molecule, and it is this intermolecular packing which is held responsible for the observed distortion. The phosphine ligand in **6α** is not so tightly packed in the crystal and the resultant molecular structure more closely approximates to the C_S symmetry expected.

Acknowledgments

We thank the EPSRC for support (KFS, BDR) and the Callery Chemical Company for a generous gift of $B_{10}H_{14}$.

References

[1] D.M. Murphy, D.M.P. Mingos, J.L. Haggitt, H.R. Powell, S.A. Westcott, T.B. Marder, N.J. Taylor and D.R. Kanis, *J. Mater. Chem.*, **3** (1993) 139;
D.A. Brown, H.M. Colquhoun, J.A. Daniels, J.A.H. MacBride, I.R. Stephenson and K. Wade, *J. Mater. Chem.*, **2** (1992) 739; and references therein.
[2] B.J. Allen et al., (eds.) *Progress in Neutron Capture Therapy for Cancer*, Plenum, New York, 1992; and references therein.
[3] F. Teixidor, J.A. Ayllon, C. Vinas, J. Ruis, C. Miravitlles and J.

Casabo, *J. Chem. Soc., Chem. Commun.*, (1992) 1279; and references therein.
[4] R. Khattar, C.B. Knobler and M.F. Hawthorne, *J. Amer. Chem. Soc.*, **112** (1990) 4962; and references therein.
[5] D.M. Schubert, W.S. Rees, Jnr., C.B. Knobler and M.F. Hawthorne, *Organometallics*, **9** (1990) 2938; and references therein.
[6] A.K. Saxena and N.S. Hosmane, *Chem. Rev.*, **93** (1993) 1081; and references therein.
[7] K.F. Shaw and A.J. Welch, *Polyhedron*, **11** (1992) 157.
[8] K.F. Shaw and A.J. Welch, *Main Group Met. Chem.*, **16** (1993) 19.
[9] B.D. Reid and A.J. Welch, unpublished results.
[10] A.I. Yanovskii, Y.T. Struchkov, V.N. Kalinin, O.M. Zurlova and L.I. Zakharkin, *Zh. Struct. Khim.*, **22** (1981) 120.
[11] G.B. Jacobsen, D.G. Meina, J.H. Morris, C. Thomson, S.J. Andrews, D. Reed, A.J. Welch and D.F. Gaines, *J. Chem. Soc., Dalton Trans.*, (1985) 1645.
[12] M.A. Bennett, T.-N. Huang, T.W. Matheson and A.K. Smith, *Inorg. Synth.*, **21** (1982) 74.
[13] R. Cramer, *Inorg. Synth.*, **15** (1974) 14.
[14] D. Drew and J.R. Doyle, *Inorg. Synth.*, **28** (1990) 346.
[15] J.M. Jenkins and B.L. Shaw, *J. Chem. Soc. (A)*, (1966) 770.
[16] R.C. Evans, F.G. Mann, H.S. Peiser and D. Purdie, *J. Chem. Soc.*, (1940) 1209.
[17] N.G. Walker and D. Stuart, *Acta Crystallogr.*, **A39** (1983) 158.
[18] G.M. Sheldrick, University of Cambridge, 1976.
[19] *International Tables for X-Ray Crystallography*, Kynoch, Birmingham, 1974, vol. 4, p. 99.
[20] R.O. Gould and D.E. Smith, University of Edinburgh, 1986.
[21] R.O. Gould and P. Taylor, University of Edinburgh, 1986.
[22] G.M. Sheldrick, University of Gottingen, 1985.
[23] M. Bown, J. Plesek, K. Base, B. Stibr, X.L.R. Fontaine, N.N. Greenwood and J.D. Kennedy, *Mag. Reson. Chem.*, **27** (1989) 947.
[24] S. Hermanek, V. Gregor, B. Stibr, J. Plesek, Z. Janousek and V.A. Antonovich, *Collect. Czech. Chem. Commun.*, **41** (1976) 1492.
[25] N. Carr, M.C. Gimeno, J.E. Goldberg, M.U. Pilotti, F.G.A. Stone and I. Topaloglu, *J. Chem. Soc., Dalton Trans.*, (1990) 2253.
[26] H.M. Colquhoun, T.J. Greenhough and M.G.H. Wallbridge, *J. Chem. Soc., Dalton Trans.*, (1985) 761.
[27] D.M.P. Mingos, M.I. Forsyth and A.J. Welch, *J. Chem. Soc., Dalton Trans.*, (1978) 1363.
[28] D.E. Smith and A.J. Welch, *Acta Crystallogr.*, **C42** (1986) 1717.
[29] G.K. Barker, M.P. Garcia, M. Green, G.N. Pain, F.G.A. Stone, S.K.R. Jones and A.J. Welch, *J. Chem. Soc., Chem. Commun.*, (1981) 652; and references therein.
[30] M.P. Garcia, M. Green, F.G.A. Stone, R.G. Somerville, A.J. Welch, C.E. Briant, D.N. Cox and D.M.P. Mingos. *J. Chem. Soc., Dalton Trans.*, (1985) 2343.
[31] X.L.R. Fontaine, N.N. Greenwood, J.D. Kennedy, J. Plesek, B. Stibr and M. Thornton-Pett, *Acta Crystallogr.*, **C46** (1990) 995.
[32] Z.G. Lewis, D. Reed and A.J. Welch, *J. Chem. Soc., Dalton Trans.*, (1992) 731.
[33] D.R. Baghurst, R.C.B. Copley, H. Fleischer, D.M.P. Mingos, G.O. Kyd, L.J. Yellowlees, A.J. Welch, T.R. Spalding and D. O'Connell, *J. Organometal. Chem.*, **447** (1993) C14.
[34] G.O. Kyd, *PhD Thesis*, University of Edinburgh, 1993.
[35] K.F. Shaw, *PhD Thesis*, University of Edinburgh, 1992.
[36] D. Hall and P.P. Williams, *Acta Crystallogr.*, **11** (1958) 624.
[37] R.J.H. Clark, V.B. Croud, H.M. Dawes and M.B. Hursthouse, *J. Chem. Soc., Dalton Trans.*, (1986) 403.
[38] C.L. Ralston, R.W. Skelton and A.H. White, *Aust. J. Chem.*, **31** (1978) 537.
[39] B. Kamenar and M. Penavic, *Inorg. Chim. Acta*, **6** (1972) 191.
[40] H.M. Colquhoun, T.J. Greenhough and M.G.H. Wallbridge, *J. Chem. Soc., Dalton Trans.*, (1979) 619.
[41] Z.G. Lewis and A.J. Welch, *Acta Crystallogr.*, **C49** (1993) 715.